T.C

(MASTER THESIS)

YAŞAR UNIVERSITY

GRADUATE SCHOOL OF NATURAL AND APPLIED SCIENCE

CARDIAC ARRHYTMIA ANALYSIS OF ECG USING HIGHER ORDER SPECTRA

Ibrahim ABDULLAHI Karaye

Thesis Advisor: Asst. Prof. Dr. Nalan ÖZKURT

Department of Electrical and Electronics Engineering

Bornova -İZMİR

2014

T.C

(MASTER THESIS)

YAŞAR UNIVERSITY

GRADUATE SCHOOL OF NATURAL AND APPLIED SCIENCE

CARDIAC ARRHYTMIA ANALYSIS OF ECG USING HIGHER ORDER SPECTRA

Ibrahim ABDULLAHI Karaye

Thesis Advisor: Asst. Prof. Dr. Nalan ÖZKURT

Department of Electrical and Electronics Engineering

Bornova -İZMİR

2014

APPROVAL PAGE

This study titled "**Cardiac Arrhythmia Analysis of ECG Using Higher Order Spectral**" and presented as Msc in Electrical and Electronics Thesis, have been evaluated in confliance with the relevant provision of the Y.U. Graduate Education and Regulation and Y.U. Institute of Education and Training Directorate. The Jury members below have decided for the defence of this thesis, and it has been decleared by concensus of the majority/votes that the candidate has succeeded in his thesis defence examination dated 25th June, 2014.

Jury members: signature:

Head.....

Rappoteur member.....

Member.....

ABSTRACT

CARDIAC ARRHYTMIA ANALYSIS OF ECG USING HIGHER ORDER SPECTRA

Ibrahim ABDULLAHI Karaye

Msc. Electrical and Electronics Engineering

Supervisor: Ass. Prof. Dr. Nalan Özkurt

June 2014

In developed countries every year hundred thousands of people die as a result of cardiac attack. The ECG is a biosignal which contains the most important information of diseases affecting the heart. Heart rate variability (HRV) analysis is an important instrument used to detect the ability of the heart to respond to normal regulatory impulses that affect its rhythm. Computer based algorithm for analysis of cardiac states is very reliable and efficient tool in diagnostics and management of arrhythmias.

The theory of nonlinear dynamic system provides some new methods to handle complex system. Like many biosignals, ECG signals are nonlinear in nature, Higher order spectral analysis (HOS) is known to be a very good tool for the analysis of nonlinear systems and produce a good noise immunity. Thus in this thesis, HOS analysis of HRV signals of normal heart rate, right bundle branch block, paced beat, left bundle branch block and atrial premature beats have been studied in order to reveal the complex dynamics of electrocardiography (ECG) signals using the tools of nonlinear systems theory. Some of the general characteristics for each of these classes in the bispectrum and bicoherence plot for visual observation have been presented. For the extraction of the R-R intervals, well known Pan-Tompkins algorithm has been used and three higher order statistical parameters of skewness, kurtosis and variance from these intervals have been computed. These features with statistical parameters fed into artificial neural network classifier (ANN) and obtained an average accuracy of 94.9%. The highest ten peaks of the cross-section of bicoherence

amplitude with their corresponding frequencies were then extracted as another set of features and fed to ANN and obtained an average accuracy of 92%. Finally, principal component analysis (PCA) has been applied to bicoherence peaks and the reduced features are fed to k nearest neighbors (KNN) search algorithm for classification. An average accuracy of 98.3% which gives a better result compared to the one using ANN with more features has been obtained.

Keywords: Arrhythmias, Higher order spectra, ECG, ANN, PCA, HRV and nonlinear system.

ÖZET

YÜKSEK DERECELİ İZGE TEKNİKLERİ İLE EKG İŞARETLERİNİN RİTM BOZUKLUĞU ANALİZİ

Ibrahim ABDULLAHI Karaye

Elektrik ve Elektronik Mühendisliği Yüksek Lisans

Danışman: Yard.Doç. Dr. Nalan Özkurt

Haziran 2014

Gelişmiş ülkelerde her yıl binlerce insan kalp krizi sonucu hayatını kaybetmektedir. EKG kalbi etkileyen birçok hastalık ile ilgili en önemli bilgileri içeren bir biyosinyaldir. Kalp hızı değişkenliği (KHD) analizi kalbin ritmini etkileyen normal düzenleyici dürtülere karşı tepkisini inceleyen önemli bir araçtır. Ritm bozukluklarının tanı ve kontrolünde kalp işaretlerini inceleyen bilgisayar tabanlı yöntemler oldukça güvenilir ve verimli araçlar olarak karşımıza çıkmaktadır.

Doğrusal olmayan dinamik sistemler teorisinde karmaşık sistemlerin analizi için birçok yeni yöntem bulunmaktadır. Birçok biyosinyal gibi EKG işareti de doğrusal değildir ve yüksek dereceli izge analizi (YDİA) yöntemlerinin doğrusal olmayan sistemlerin analizinde çok iyi bir yöntem olduğu ve gürültüye karşı dayanıklılığının da yüksek olduğu bilinmektedir. Bu nedenle, bu tezde normal, sağ dal bloğu, kalp pilli, sol dal bloğu ve atriyal prematüre atım KHD işaretlerinin karmaşık dinamiklerinin açıklanabilmesi için doğrusal olmayan sistem teorisi araçlarından YDİA yöntemleriyle analizi üzerine çalışılmıştır. Bu sınıfların ikiz izge ve ikiz eşfaz çizimlerindeki genel karakteristikleri görsel karşılaştırma için sunulmuştur. R-R aralıklarının belirlenmesi için Pan-Tompkins algoritması kullanılmış, bu özniteliklerin yüksek dereceli istatistiksel parametreleri olan çarpıklık, basıklık ve varyansları hesaplanmıştır. Bu öznitelikler yapay sinir ağı ile sınıflandırılmış ve %94.9 ortalama doğruluk oranı elde edilmiştir. İkiz eşfaz eğrilerinin kesitlerinin en büyük on tepesinin genlik ve frekanslarından elde edilen

özniteliklerin yapay sinir ağlarıyla sınıflandırılmasının ardından ise %92 ortalama doğruluk elde edilmiştir. Son olarak ikiz eşfaz tepeleri özniteliklerine temel bileşen analizi yapılarak veri boyutu azaltılmış ve k-en yakın komşuluk algoritması ile sınıflandırılmıştır. Bu sınıflandırıcı %98.3 doğrulukla yapay sinir ağlarına göre daha iyi bir başarım sağlamıştır.

Anahtar Kelimeler: Ritm bozuklukları, yüksek dereceli izge, EKG, yapay sinir ağları, temel bileşen analizi, KHD ve doğrusal olmayan sistemler

ACKNOWLEDGEMENTS

I would like to express my appreciation to my supervisor Asst. Prof. Dr. Nalan Özkurt, for her guidance, support, advice, patience and valuable suggestions in achieving this task.

I would also like to thanks my colleagues, especially Sani Saminu for his valuable advice and suggestion

I would also like to thank all members of the department for their support.

I would also like to thank my parents for their support and prayers.

I would also like to thank the governor and good people of Kano state for their financial support.

Last but not least, I would like to thank my wife who endured my absence throughout this period and my new born baby who is yet to meet me due to this research.

TEXT OF OATH

I declared and honestly confirmed that my study “Cardiac arrhythmia analysis of ECG signal using Higher order spectral” and presented as a master’s thesis, has been written without any assistance inconsistent with scientific ethics and traditions, that all sources from which I have benefitted are listed in the bibliography, and that I have benefitted from these sources by means of making references.

Ibrahim Abdullahi Karaye

TABLE OF CONTENTS

INDEX OF FIGURE

INDEX OF TABLE

INDEX OF ABREVIATIONS

ANN	Artificial neural network
ANFIS	Adaptive neuro-Fuzzy Interference
ANS	Autonomous Nervous System
AR	Autorgressive
ARMA	Autoregressive Moving Average
APB	Atrial Premature Beat
APC	Atrial Premature Contraction
AV	Atrio Ventricular
BIH	Beth Israel Hospital
BPA	Back Propagation Algorithm
DC	Direct Current
DDFT	Double Discrete Fourier Transform
DFT	Discrete Fourier Transform
ECG	Electrocardiogram
EEG	Electroencephalogram
EMG	Electromayogram
FFT	Fast Fourier Transform
FN	False Negative
FP	False Positive
HOS	Higher Order Spectra
HOSA	Higher Order Spectral Analysis

HRV	Heart Rate Variability
ICU	Intensive Care Unit
ICCU	Intensive Coronory Care Unit
kHZ	Kilo Hertz
KNN	K-Nearest Neighborhood
LA	Left Arm
LBBB	Left Bundle Branch Block
MA	Moving Average
MIT	Massachusets Institute of Technology
PAC	Premature Atrial Contraction
PCA	Principal Component Analysis
PDF	Probability Density Function
RA	Right Arm
RBBB	Right Bundle Branch Block
SA	Sino Atrial
SNR	Signal to Noise Ratio
TN	True Negative
TP	True Positive
1D	1 dimensional
3D	3 Dimensional

CHAPTER 1

INTRODUCTION

Computer technology has an important role in structuring biological systems. The explosive growth of high performance computing techniques in recent years, with regard to the development of good and accurate models of biological systems, has contributed significantly to new approaches of fundamental problems of modeling linear and nonlinear behaviors of biological systems.

A complex system like cardiovascular system cannot be linear in nature and by considering it as a nonlinear system, can lead to better understanding of the system dynamics. Recent studies have also stressed the importance of nonlinear techniques to study HRV in issues related to both health and diseases.

The progress made in the field using measures of chaos has attracted the scientific community to apply these tools in studying physiological systems, and ECG is no exception.

A great deal of attention has been focused recently on the extraction of dynamical information from chaotic time series (Broomhead et al, 1986; Simm et al, 1987; Denker et al, 1986). Chaos is the state in which a nonlinear dynamical system exhibits bounded motion, with exponential sensitivity to initial conditions, in that initially neighboring state of a chaotic system diverges exponentially as the system evolves forward in time (Guckenheimer et al, 1983).

Recently, the nonlinear techniques have been used to analyze physiological signals: heart rate, nerve activity, renal blood flow, arterial pressure, EEG and respiratory signals (Kannathal et al, 2004; Acharya et al, 2004; Garrat et al, 2003; Yuru et al, 2004). To investigate the time-varying spectral characteristics

of the underlying process, most of the methods often begin by computing the time variation of the common statistical properties of the process (Roberto et al, 1995; Kaplan, 1999; Laurent et al, 1998). However, these methods all assume that piecewise first-order or second-order stationarity is satisfied for each segment of the observation after segmentation.

In practice, many medical signals show significant nonlinear and non-Gaussian characteristics, such as the presence of nonlinear effects of phase coupling among the signal frequency component (Shan et al, 2000; Ning, 1993; Ning et al, 1990; Husur et al, 1997). The methods based on lower order statistics or spectral analysis fail to deal with the nonlinearity and non-Gaussianity of the processes, but higher-order spectral techniques (HOS) allow us to effectively process these signals to obtain their higher order statistics.

For many decades correlation and power spectrum have been primary tools for digital signal processing applications in the biomedical field. The information contained in the power spectrum is essentially that of the autocorrelation sequence, which is sufficient for complete statistical descriptions of Gaussian signals of known means.

However, there are practical situations where one needs to look beyond autocorrelation of a signal to extract information regarding deviation from Gaussianity and the presence of phase relations. Higher order spectral techniques, also known as polyspectra, are spectral representations of higher order statistics, i.e. moments and cumulants of third order and beyond. HOS can detect deviation from linearity, stationarity and non Gaussianity from the signal. Most of the biomedical signals are non-linear, non-stationary and non-Gaussian in nature and therefore it can be advantageous to analyze them with HOS compared to the use of second order correlations and power spectra.

HOS have been applied to many applications such as in oceanography (Hasselman et al, 1963), 1D pattern recognition (Chadran et al, 1991b; Chadran

et al, 1991a), chaotic signal characterization (Chadran et al, 1993b), array signal processing (El-Jaroudi et al, 1994), telecommunication (El-Khamy et al, 1995), ultrasound image processing (Abeyratne et al, 1997), detection of mines from sonar images (Chadran et al, 2002), study of machine faults (Jang et al, 2004), speaker verification (Chadran et al, 2004), recognition of viruses from electron microscopic images (Ong et al, 2005), termite detection (La Rosa et al, 2007), analysis of bio signals like the ECG (Khadra et al. 2005) and identification of cardiac ischemia (Rama et al. 2012). Rama Valupadasu in his work has identified the difference between cardiac ischemia and the normal heart rate beat. In which he found the higher order statistical parameters of the normal and compare it with the ischemic patient, and conclude that the phase correlation of a normal person is low while that of ischemic person is high.

The use of non-linear features motivated by higher order spectra (HOS) has been reported to be a promising approach to analyze the non-linear characteristics of the bio signals. Thus, in this work, the applications of Higher order spectral (HOS) for ECG signals have been discussed.

1.1 Motivation

Electrocardiography (ECG) has a basic role in cardiology since it consists of effective simple non-invasive low cost procedure for the diagnosis of cardiac disorders that have high epidemiological incidence and a very relevant for their impact on patient life and social cost. Cardiac rhythm disturbances are considered to lead to life threatening conditions. Thus the detection of abnormalities in intensive care patients is very essential and critical.

Recently, a lot of researches have been done for automating the abnormality detection applying various engineering methods and non-conventional techniques, especially in the scenario of continues monitoring of ECG in intensive care units (ICU's). Computer and automatic analysis of ECG and abnormality detection is very helpful, as it will be an aid to the cardiologist in

the absence of the doctor. It will also help the doctor to diagnose and prescribe faster in case of emergency conditions.

Designing a low cost, high performance, simple to use and portable devices for ECG offering a diagnostic feature seems to be a global pursuit. Such equipment should embed and integrate several techniques of data analysis such as signal processing, pattern recognition and detection, decision support and human computer interactions. Thus computerized methods are to be used for detection and classification of abnormalities.

Therefore, in this study, a cardiac arrhythmia analysis method which may be used for a wearable ECG analysis system has been proposed by using higher order statistical methods.

1.2 Objectives and Contributions

The present work is to perform nonlinear time series analysis on ECG and use of classification techniques such as neural networks, k-neighbors etc. to classify and model the signals. The milestones achieved in this work are

- To establish an appropriate and relevant set of HOS features to detect various cardiac abnormalities from the ECG signals.
- To use different classifiers for classification of the ECG for the abnormalities based on the features chosen.
- To propose unique HOS plots for different cardiac arrhythmias and normal that could aid visual interpretation.

The contributions derived from this work are summarized below:

- A new set of features based on HOS and statistics were used for the different cardiac arrhythmias.
- Evaluation of features extracted using HOS analysis techniques for detection of cardiac abnormalities.

1.3 Outline of Thesis

The outline of this report is as follows:

Chapter 1 gives the background of what the thesis intended to achieve and some literature reviews about the methods used in the arrhythmia classification.

Chapter 2 gives brief explanations of the physiological anatomy of the heart and the arrhythmias used in this work.

Chapter 3 gives the general discussion about the ECG signal; its leads, acquisitions, steps in its analysis and QRS detection technique used in the thesis.

Chapter 4 describes the higher order spectral technique, its estimation, the statistical features, bispectrum and bicoherence plots.

Chapter 5 describes the results obtained from this work and compares it with other similar works.

Chapter 6 gives the summary, conclusion and the future works.

CHAPTER 2

PHYSIOLOGICAL BACKGROUND

In order to understand the function of the heart and heart diseases well, basic knowledge of the functional anatomy of the heart is necessary. In this chapter, a general overview of the heart circulatory system, the conduction system of the heart, the heart rate variability concept, heart problems, and the brief information about the four arrhythmias used in this study with their related literature will be given.

2.1 The Circulatory System

The circulatory system carries nourishment and oxygen (O2) to, and waste and carbon dioxide (CO2) from, the tissues and organs of the body. The system can be considered as a closed loop hydraulic system (Webster, 1998).

2.1.1 Elementary Circulatory System

The simplified form of the human circulatory system is shown in Fig. 2.1. The heart can be considered as a pump to move blood through vessels called arteries and veins. Blood is carried away from the heart in arteries and is brought back to the heart in veins.

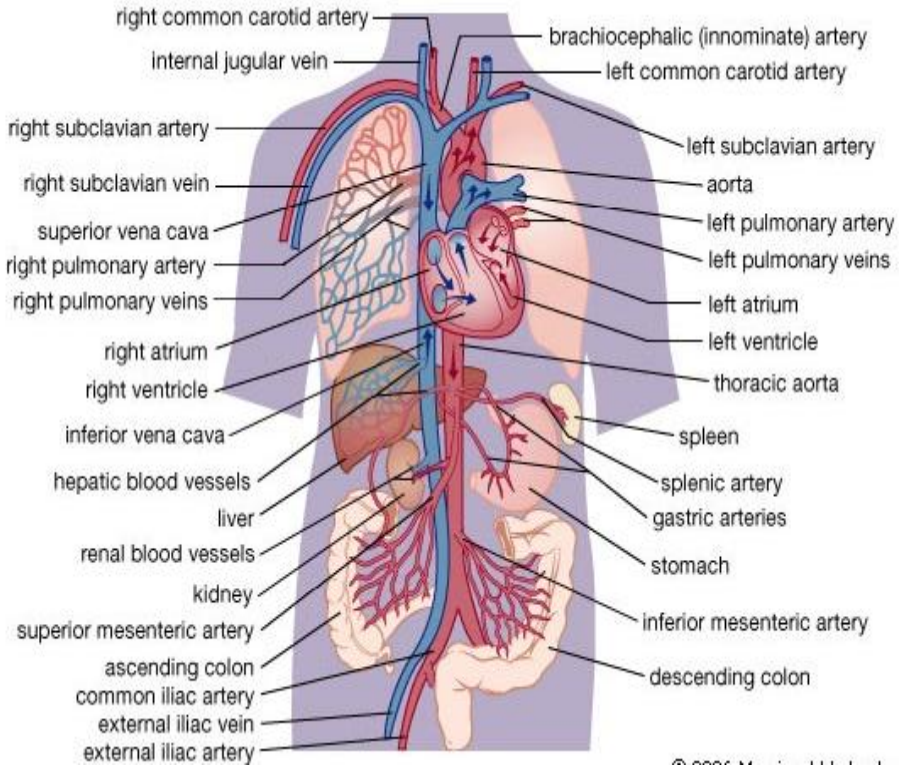

Fig 2.1.The circulatory system of the heart (Webster, 1998)

When blood is circulated through the body, it carries O2 and nutrients to the organs and tissues and returns carrying CO2 to be excreted through the lungs and various waste products to be excreted through the kidneys. The deoxygenated blood is returned to the right side of the heart via the venous system.

2.2 The Heart

The rate at which the heart beats in the absence of neurohumoral (nerve chemical) influences is referred to as the intrinsic heart rate. In heart transplant patients, the SA node - and hence the heart as a unit - cycles close to an intrinsic rate of 90-95 beats per minute (bpm). However, in a normal healthy individual, the beating of the heart is modulated to a slower rate by the influence of extrinsic nervous influence on the SA and AV nodes by the autonomic nervous system (ANS). Other factors such as temperature change and tissue stretch may also influence the discharge frequency of the SA node although autonomic control is the principal controller (Cooper, Lei, Cheng, & Kohl, 2000). In addition, during atria pacing autonomic neural activity

associated with respiration and blood pressure appears to dynamically modulate AV conduction with respiratory effects predominating at low heart rates and blood pressure effects at high heart rates (Warner & Loeb, 1986). The quantity of blood pumped by the heart (cardiac output) may be considered as the product of heart rate and stroke volume. Therefore, cardiac activity is related to both regulation of pacemaker activity and myocardial performance, with heart rate being regulated mainly by the ANS. However, baroreceptor, chemoreceptor, pulmonary inflation, atrial receptor (Bainbridge) and ventricular receptor reflexes can also regulate heart rate (Berne & Levy, 1997).

Figure 2.2 below, shows the basic structure of the heart and the direction of flows of blood as well as the connected blood vessels. There are four valves in the human heart. The valves between the right atrium and the right ventricle are known as the tricuspid valve. It gets its name from the fact that it is formed of three cusp-shaped flaps of tissue arranged so that they will shut off and block passages of blood in the reverse direction(from ventricles back to atrium). The second valve which is between the right ventricle and the pulmonary artery is named for its shape: Semilunar (half moon) valve. It prevents reverse flow (regurgitation) of blood from the pulmonary artery to the right ventricle. Then, blood returning to the heart from the lungs must pass through the left atrium and the mitral valve (also known as a bicuspid valve for its shape) to the left ventricle. The last valve is the aortic-valve. Its shape is similar to the pulmonary valve and prevents regurgitation of blood from the aorta back to the left ventricle (Webster, 1998).

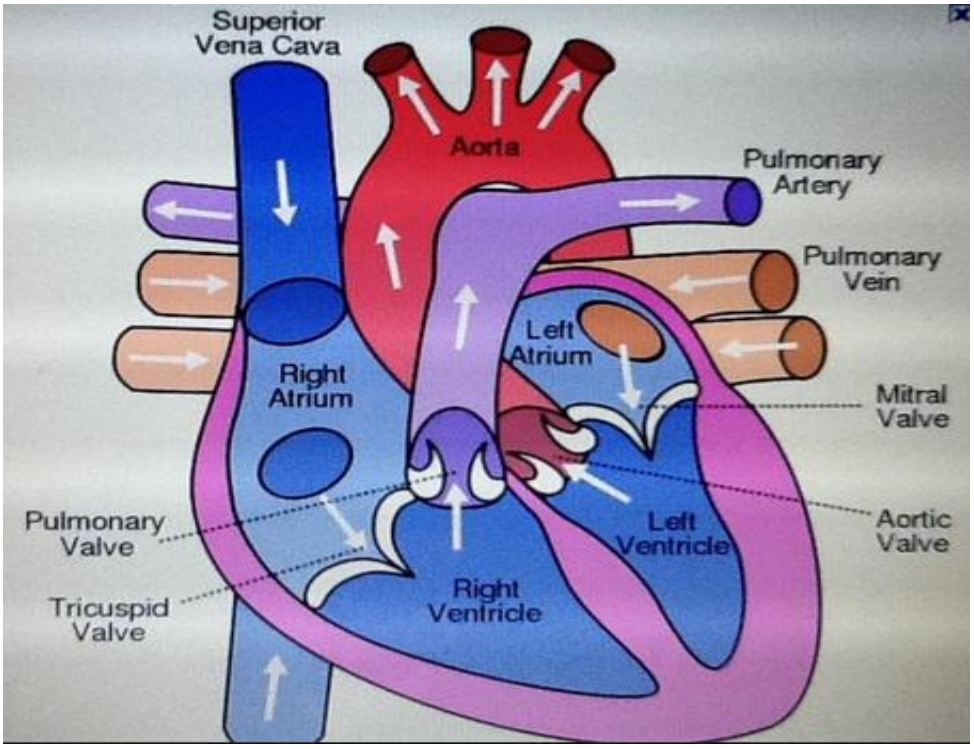

Fig 2.2 The direction of blood flow in the heart (Webster, 1998)

The heart serves as a pump because of its ability to contract under electrical stimulus. When an electrical triggering signal is received, the heart will contract, starting in the atria, which undergo a shallow, ripple-like contracting motion. A fraction of a second later, the ventricles also begin to contract, from the bottom up, in a motion that resembles wringing out a dishrag or sponge. The ventricular contraction is known as ***systole*** and the ventricular relaxation is known as ***diastole***.

2.2.1 Electroconduction System of the Heart

The conduction system of the heart (Fig. 2.3) consists of the sinoatrial (SA) node, bundle of His, atrioventricular (AV) node, the bundle branches, and Purkinje fibers.

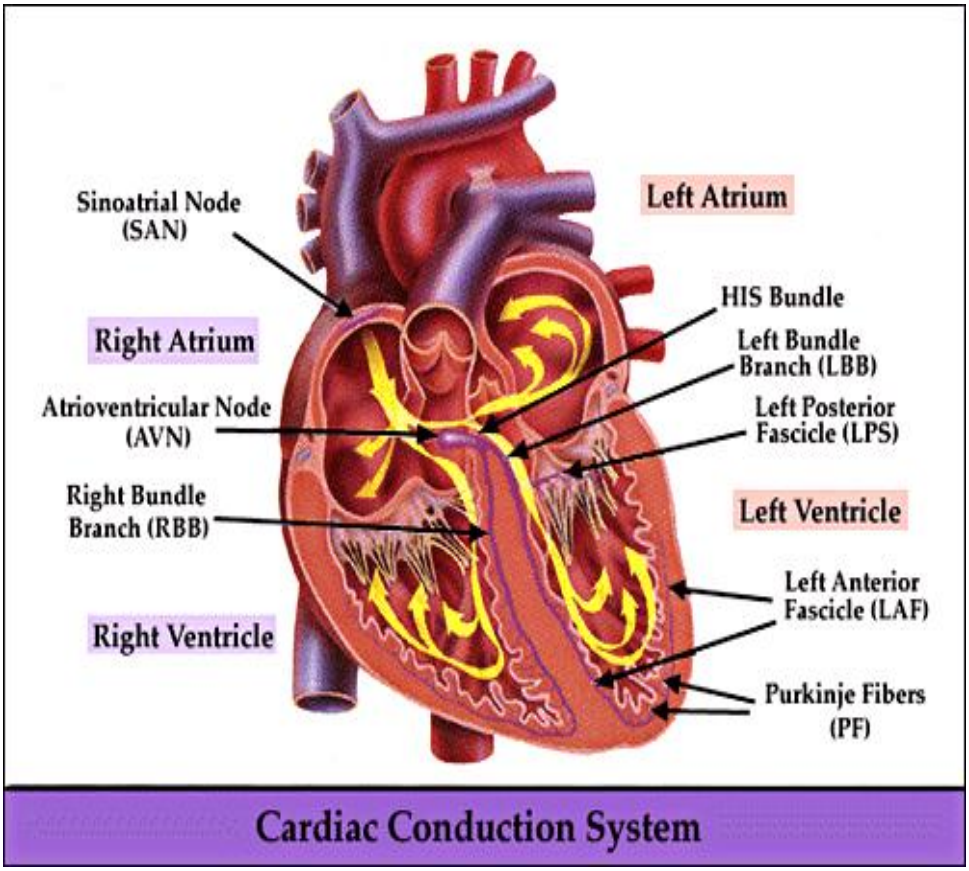

Figure 2.3 Conduction system of the heart (Webster, 1993).

The SA node serves as a pacemaker for the heart, and it provides the trigger signal. It is a small bundle of cells located on the rear wall of the right atrium, just below the point where superior vena cava is attached. The SA node fires electrical impulses through the bioelectric mechanism. It is capable of *self-excitation* (firing on its own).

When the SA node discharges a pulse, the electrical current spreads across the atria, causing them to contract. Blood in the atria is forced by the contraction through the valves to the ventricles.

There is a band of specialized tissue between the SA node and the AV node, however, in which the velocity of propagation is faster than it is in atrial tissue. This internal conduction pathway carries the signal to the ventricles.

It would not be desirable for the ventricles to contract in response to an action potential before the atria are empty of their contents. A delay is needed, therefore, to prevent such an occurrence; this is the function of the AV node. The action potential will reach the AV node 30 to 50 ms after the SA node

discharges, but another 110 ms will pass before the pulse is transmitted from the AV node. The AV node operates like a delay line to retard the advance of the action potential along the internal electro conduction system toward the ventricles.

Conduction into the bundle branches is rapid, consuming only another 60 ms to reach the furthest Purkinje fibers. The muscle cells of the ventricles are actually excited by the Purkinje fibers. The action potential travels along these fibers at a much faster rate, on the order of 2 to 4 m/s. The fibers are arranged in two bundles, one branch to the left and one to the right.

2.3 Heart Problems

The physician uses the ECG and other tests to determine the gross condition of the heart. Although a complete discussion of heart problems is beyond the scope of this work, some of the more common problems are discussed below in generalized terms.

The heart is a muscle and must be per-fused with blood to keep it healthy. Blood is supplied to the heart through the coronary arteries that branch off from the aorta just before it joins the heart. If an artery bringing blood to the heart becomes partially or totally blocked off, the area of the heart served by that vessel will suffer damage from the loss of the blood flow. That area of the heart is said to be infarcted and is dysfunctional. This type of damage is referred to as a myocardial infarction, another term for heart attack.

Another class of heart problem is cardiac arrhythmias. These are abnormal heartbeat rhythms and may be seen as ECG changes. Conditions under this classification include extremes in heart rate, premature contractions, heart block, and fibrillation.

The human heart rate varies normally over a range of 60-110 beats/min (bpm). Rates, faster than this, are called tachycardia. Various authorities list slightly different figures as the threshold for defined tachycardia, but most list 120 bpm, with the range being 110 to 130 bpm.

The opposite condition, when a heart rate is too slow, is called bradycardia, and again different sources list slightly different thresholds, but all are within the 40- to 60-beats/min range.

2.3.1 Normal Heart ECG

A normal heart beat is said to occur when a P wave exist for every QRS complex and each P wave is the same distance from the QRS complex-less than 0.20 seconds, all QRS complexes are the same size and shape and point in the same direction. Each QRS is the same distance from the T waves and the QRS, the duration is 0.10seconds or less. Heart rate will be varying in the range of 60-100 beats/minutes and is rhythmic.

2.3.2 Right Bundle Branch Block (RBBB)

Bundle branch block is a condition in which there's a delay or obstruction along the pathway that electrical impulses travel to make your heart beat. The delay or blockage may occur on the pathway that sends electrical impulses to the left or the right side of your heart. When the activation of the right ventricle is delayed, which causes the right ventricle to contract later than the left ventricle then is referred to right bundle block. A RBBB has the following wave form characteristics:

- A complete RBBB has a QRS of 0.12sec or more
- It has a prolonged right ventricular activation time or QR interval of 0.03sec or more in V1-V2
- The delayed right ventricular activation produces a secondary R wave (R’) in the right precordial leads (V1-3) and a wide, slurred S wave in the lateral leads
- Delayed activation of the right ventricle also gives rise to secondary repolarization abnormalities, with ST depression and T wave inversion in the right precordial leads.

- If the QRS duration is between 0.10sec and 0.11sec then it is incomplete RBBB

2.3.3 Left Bundle Branch Block (LBBB)

In this condition, activation of the left ventricle is delayed, which causes the left ventricle to contract later than the right ventricle. It has the following characteristics:

- A complete LBBB has a QRS of greater than 0.12sec
- Normally the septum is activated from left to right, producing small Q waves in the lateral leads.
- As the ventricles are activated sequentially (right, then left) rather than simultaneously, this produces a broad or notched ('M'-shaped) R wave in the lateral leads.

2.3.4 The Paced Beat

This is an artificial beat from a device called pacemaker. A pacemaker is a treatment for dangerously slow start beats, without treatment, a slow heart beat can lead to weakness, confusion, dizziness, fainting, shortness of breath and death. Slow heart beat can be the result of metabolic abnormalities or occur as a result of blocked arteries to the heart conduction system. This conduction can often be treated and a normal heart beat can resume. Slow heart beat can also be a side effect to a certain medications in which case discontinuation of the medicine or a reduction in dose may correct the problem. The paced beat has the following features:

- A Normal pacemaker rhythm can result in absent pacing activity, irregular pacing and absence of pacing spikes.
- Ventricular pacing spikes follow each P wave, most easily seen in V3-V6

- Tiny pacing spikes are also visible in I, aVR and V1.
- There is presumably an underlying complete heart block or high –grade 2nd degree AV block, as the native P waves do not capture the ventricles.

2.3.5 The Atrial Premature Beat (APB)

Premature contractions occur when an area of the heart becomes irritable enough to produce a spurious action potential at a time between normal beats. The action potential spreads across the myocardium in much the same manner as the regular discharge. Beats occurring at improper times are called ectopic beats. If it results in atrial contraction, then it is an atrial premature contraction (APC), and if in the ventricle, a ventricular premature contraction (VPC), and both the two can be referred to as atria premature beats. It has the following characteristics:

- They are premature
- They are *ectopic*
- They are *narrow complexes*
- There is a *compensatory pause* after the PAC
- An abnormal (non-sinus) P wave is followed by a QRS complex.

CHAPTER 3

ECG PREPROCESSING TECHNIQUES

3.1 General Overview

Over the past four decades, analysis of electrocardiogram (ECG) has been one of the major research interests in biomedical signal processing. One reason for this is the growth in the cardiac health care activities all over the world, and the other is the rapid advance in digital computer technology. Computers in medical care essentially mimic the clinician in the detection of disease states from bio-signals. Computers also prove to be a more reliable replacement of clinician in applications involving routine and tiresome work, such as patient monitoring in intensive coronary care unit (ICCU) or processing of large amount of information as in (Holter,1961). Quantitative assessment and diagnostic results is very helpful in clinical therapy, as subjective interpretations are prone to a wide range of inconsistencies and inaccuracies. Thus, in areas heavily dependent upon quantitative assessment, accuracy and speed, computer based analysis is very useful in diagnostics. The advances made in the fields of electrocardiography, sonography, imaging, laser technology and many others have given a new dimension to health care in the 20th century and have a bigger role to play in the coming years.

3.2 Electrocardiography

The electrocardiogram deals with the electrical activity of the heart. The action potential generated in the SA node stimulates the muscles fibers of the myocardium, causing them to contract. When the muscles are in contraction, it is shorter, and the volume of the ventricular chamber is less, so blood is squeezed out. The contraction of so many muscles cells at one time creates a mass electrical signal that can be detected by placing sensors at the limb extremities of the subject. This electrical discharge can be mathematically plotted as a function of time, and the resultant waveform is referred to as the electrocardiogram (ECG).

Figure 3.1 below shows ECG waveform of a healthy individual.

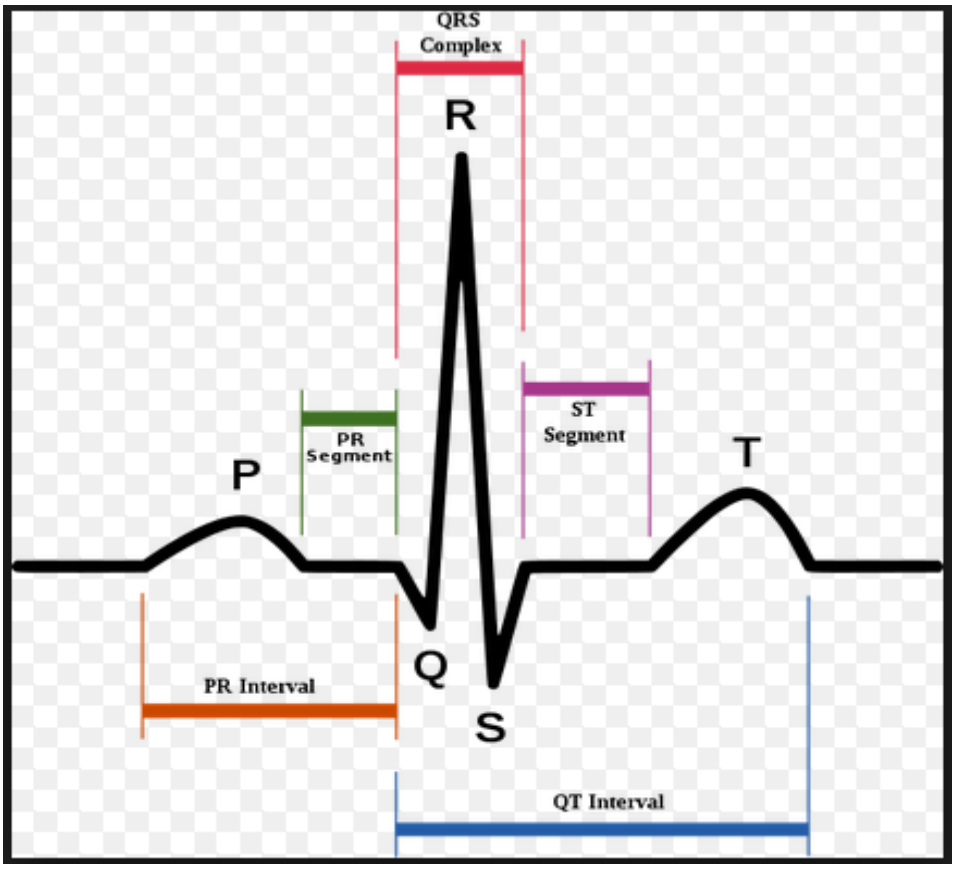

Figure 3.1 ECG waveform of a healthy individual (J. Malmivauo et al; 1995)

3.2.1 Leads

The ECG is recorded on electrocardiographic leads. The term "lead" refers to a measurement configuration of electrodes. Three bipolar limb leads of the frontal plane are connected between limbs (Fig. 3.2). Taking lead I as an example, the negative terminal electrode is connected to the right arm (RA) and the positive terminal electrode to the left arm (LA). These three limb leads constitute Einthoven's triangle. If any two of the three electrocardiographic leads are known, the third one can be determined mathematically from the first two (Einthoven's law). The other three unipolar frontal leads are aVR (on the right arm), aVL (on the left arm) and aVF (on the foot), which are usually called augmented unipolar leads, measuring the potential difference on a limb

with respect to a reference point formed by the two resistors between the electrodes on the other two limbs (Fig. 3.2).

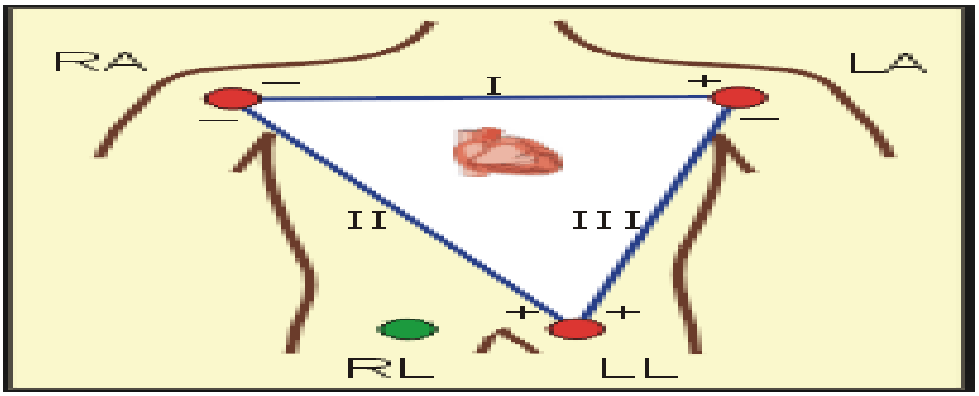

Fig.3.2 Directions of standard limb lead vectors (J. Malmivuo et al, 1995)

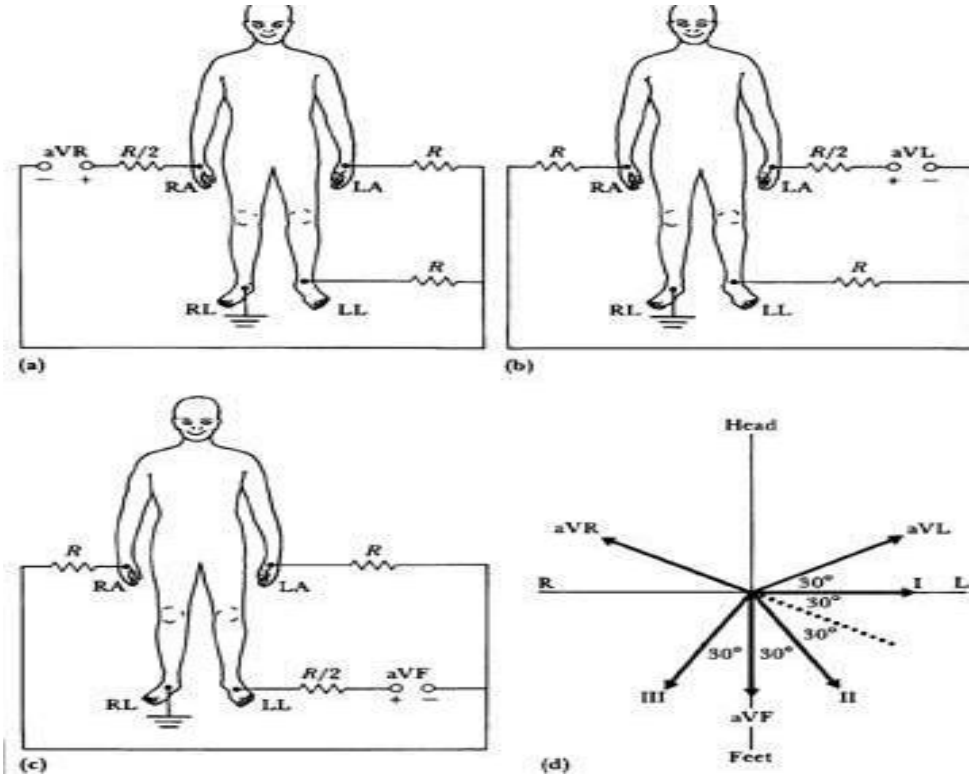

Fig.3.3 (a), (b), (c) Connections of electrodes for the augmented limb leads, (d) Vector diagram showing the directions of limb lead vectors in the frontal plane (J. Malmivuo et al; 1995)

The six precordial leads, VI-V6, are unipolar and measure the cardiac vector projection on the horizontal plane (Fig. 3.3). These precordial leads are measured with respect to the Wilson's central terminal, which is formed by a

three-resistor network in Fig. 3.3, yielding an average of right and left arms and left leg.

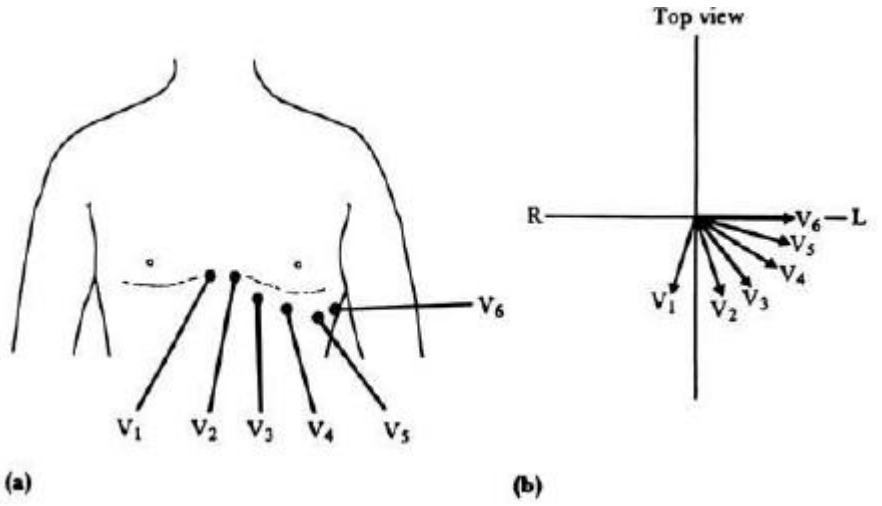

Fig.3.4 (a) Positions of precordial leads on the chest wall, (b) Directions of precordial lead vectors in the transverse plane (J. Malmivauo et al; 1995)

In order to use the surface ECG to diagnose abnormalities, it is important to know the normal characteristics of the ECG. A sample of a normal 12 lead ECG (10 s strip, paper speed 25 mm/s) is demonstrated in Fig. 3.2. For a normal ECG, typical P wave duration is less than 0.11 s (equivalent to 2.75 mm measured on the above figure), and the morphology does not include any notches or peaks. The P wave is normally positive in leads I, II, aVF, V4 and V6, and negative in aVR. It can be positive, negative, or biphasic in all other leads. The QRS complex duration is normally less than 0.12 s, and the morphology differs in different leads. In some leads there exist downward deflections of Q and S waves, and a large upward deflection of R wave in between as shown in Fig. 3.3. The normal morphology of the T wave is rounded and asymmetrical. It is positive in leads I, II, V3 and V6, and negative in aVR. The polarity may vary in leads III, V1 and V2. Typically the P-R interval is 0.18-0.2s, and R-R interval is 0.6-1.0s (Yanowitz, 2006).

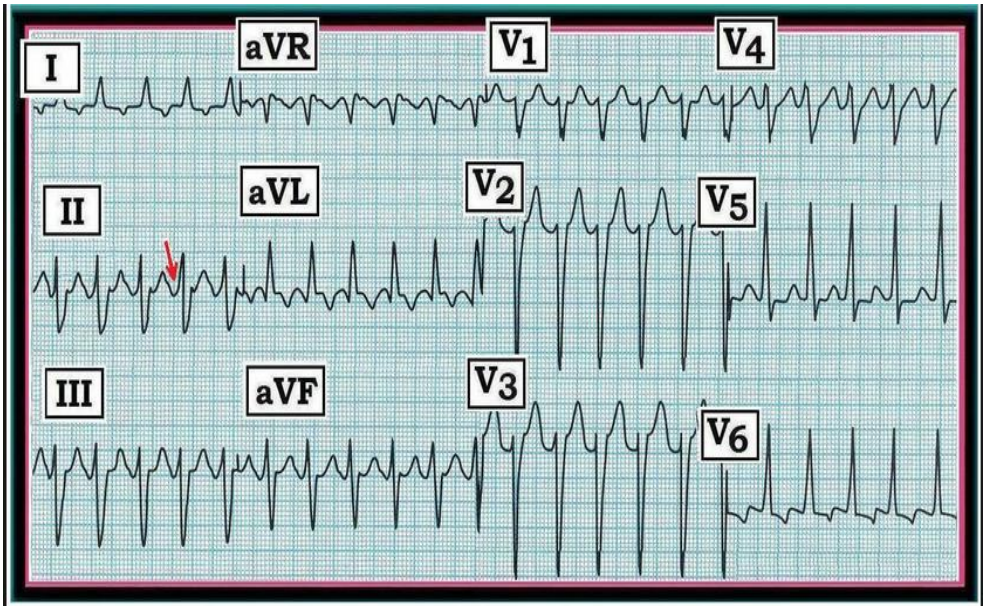

Figure 3.5 Example of 12-lead ECG record (J. Malmivauo et al; 1995)

3.2.2 Data Acquisition

The source of ECG's signal in this thesis is obtained from the MIT-BIH Arrhythmia database, which is a set of over 4000 long term Holter recordings were obtained from in patients. The database contains 23 records (numbered from 100 to 124 inclusive with some numbers missing) chosen at random from this set, and 25 records (numbered from 200 to 234 inclusive, again with some numbers missing) selected from the set to include a variety of rare but clinically important phenomena that would not be well-represented by a small sample of Holter recordings. Each of the 48 records is slightly over 30 minutes long.

Records in the second group were chosen to include complex ventricular, junctional, and supraventricular arrhythmia and conduction abnormalities. Several of these records were selected because of the rhythm, QRS morphology variation, or signal quality might be expected to present significant difficulty to arrhythmia detector; these records have gained considerable notoriety among database users. The subject was 25 men aged 32 to 89 years, and 22 women aged 23 to 89 years (Mark, 1992). In this work we used ECG records of 100,101,102,111,118 and 232 from the database.

3.2.3 Steps in ECG Analysis

The major steps in the analysis of ECG signals are:

- Noise elimination from ECG using noise filtering techniques.
- Cardiac cycle detection by detecting QRS complex.
- Detection of significant characteristics point in ECG signal.
- Formulation of characteristics features set.

Noise filter removes and reduces the noise components from various sources in the ECG signal.

Cardiac cycle detection involves detecting the QRS complex peak corresponding to each beat. QRS complex detection algorithm (Pan,et, al, 1985).

ECG characteristics point detection involves determining of significant points in the ECG for feature extraction; it includes the detection of QRS complex onset and offset, ST segment and T peak detections.

Feature set formulation includes formulation and selection of characteristics features such that they significantly relate to the abnormalities. Additional features are extracted by performing complexity analysis on the signal**.**

3.3 Signal Pre-processing

Signal processing can be defined as the manipulation of a signal for the purpose of extracting information from the signal or producing an alternative representation of the signal. There are numerous specific motivations for signal processing, but many fall into following three categories. First is to remove unwanted signal components that are corrupting the signal of interest. Second is to extract information by rendering it in a more obvious or more useful form and third is to predict future values of the signal in order to anticipate the behavior of its source.

This thesis, at signal pre-processing step is focused on noise removal and after this step processing of the signal will continue with QRS detection and feature extraction steps. ECG beat detection systems have to be designed in a way that they are capable of working in a noisy hospital environment. ECG signal is normally corrupted with different types of noise.

To obtain useful information from raw signals, they are first processed to remove the noise. Although our system will not be working on real time patient recorded signals, the ECG data that got from MIT-BIH database may also contain some noise (Figure 3.6) so we also have to pre-process the signal and remove the noise.

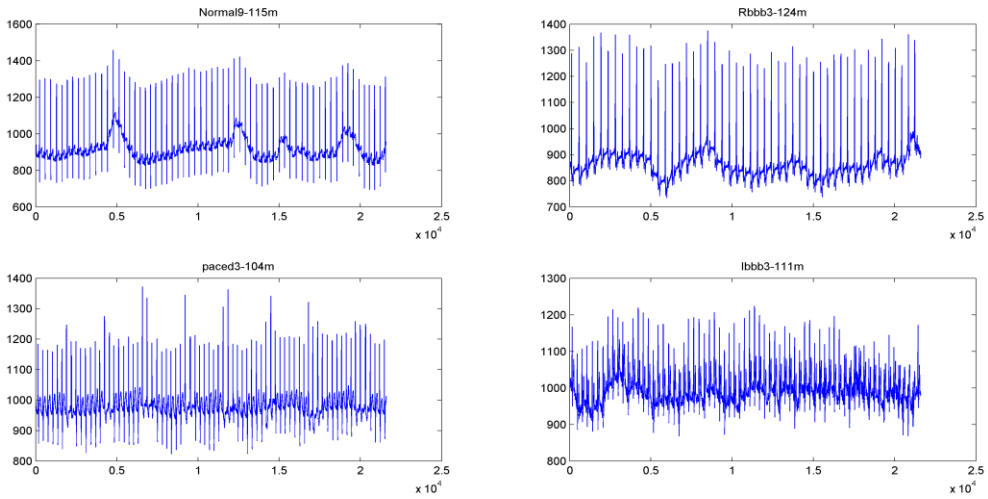

Figure 3.6: A Section of noisy ECG Records Obtained from MIT-BIH Database

The ECG consists of three basic waves, P, QRS and T. These waves correspond to the field induced by specific electrical phenomena on the cardiac surface, namely the atrial depolarization (P wave), the ventricular depolarization (QRS complex) and the ventricular re-polarization (T wave). The ECG does not look the same in all leads of the standard 12 leads system used in clinical practice. The polarity and the shape of the ECG constituents' waves are different depending on the lead that is used.

In a normal cardiac cycle, the P wave occurs first, followed by the QRS complex and then the T wave .The sections of the ECG between the waves and complexes are called segments. The ECG is characterized by three segments namely; the PR segment, The ST segment and the TP segment. The characteristics time period in the ECG are the PR interval, the RT interval and the R-R interval.

Usually ECG signals are contaminated by various kind of noise. Various types of noise that are contaminating the ECG signals are discussed below:

- Power line interference: This noise consists of 60/50 Hz pickup and harmonics that can be modeled as sinusoids and combination of sinusoids. According to Friensel et al (Friensel et al; 1990), the frequency content of this kind of noise is 60/50 Hz with harmonics and the amplitude is 50% of peak-to-peak ECG amplitude.

- Electrode contact noise: This is a transient interference caused by loss of contact between the electrode and the skin, which can be permanent or intermittent. The switching action can result in large artifacts since the ECG signal is usually capacitive coupled to the system. This type of noise can be modeled as a randomly occurring rapid baseline transition that decays exponentially to the baseline and has a superimposed 60Hz component. According to Friensel et al (Friensel et al; 1990), the duration of the noise signal is 1sec and the amplitude is the maximum recorded output with the frequency of 60Hz.

- Motion artifact: This is transient baseline changes in the electrode skin impedances with electrode motion. The shape of the baseline disturbance caused by the motion artifacts can be assumed to be biphasic signal resembling one cycle of a sine wave. The peak amplitude and duration of the artifacts are variables. The duration of this kind of signal is 100-500ms with amplitude of 500% peak-to-peak ECG amplitude.

- Muscle contraction: This noise caused artifact millivolt level potentials to be generated. They can be assumed to be transient bursts of zero mean, bond

limited Gaussian noise. The variance of the distribution may be estimated from the variation and duration of the bursts. The standard deviation of this kind of noise is about 10% of the peak-to-peak ECG amplitude, with duration of 50ms and the frequency content being DC and up to 10 KHz.

- Baseline wander: This noise causes problems in the detection of ECG peaks. For example, due to the wander, the T peak could be higher than R peak, and it is detected as an R instead. Low frequency wander of the ECG signal can be caused by respiration or movement of patients. The drift of the base line with respiration can be represented as a sinusoidal component and the frequency of the respiration added to the ECG signal. The variation could be reproduced by amplitude modulation of the ECG by the sinusoidal component that is added to the base line. The amplitude is 15% of the peak-to-peak ECG amplitude and the base line variations is 15% of ECG amplitude at 0.15 to 0.3 Hz. The noise artifacts should be removed from ECG before extracting the characteristics features. Noise removal is accomplished by passing the cardiovascular signal through a filter whose cut off frequency is a function of the noise frequency.

3.4 Noise Filtering Technique

To remove unwanted noise from raw ECG signals four levels of filtering is applied to ECG records; DC component removing, 10 point moving average (low pass) filter, derivative based (high pass) filter and a comb filter.

3.4.1 Removing DC Components in ECG Signal

As it can be clearly seen from Figure 3.6, ECG signals taken from MIT-BIH database contain baseline (sections of ECG where there is no electrical activity of heart) amplitudes higher than zero. In this step by subtracting the mean of the signal from itself, the unwanted dc component is removed and the signal baseline amplitude is pulled back to level zero.

$$ECGSignal = ECGSignal - mean(ECGSignal) \quad (3.1)$$

3.4.2 Removing Low Frequency and High Frequency Noise

ECG data used for the system contains low and high frequency noise components that may be caused by the sources explained in the previous pages. Before the design of the software both frequency domain and time domain filters were tested for noise removal. It is observed that time domain filters provide better noise removal on the signals obtained from MIT-BIH database than frequency domain filters (Butterworth filters in our case). Because of this and since most of the noise present in the database is random noise, time domain filters were chosen to filter unwanted high and low frequency noise.

To remove high frequency random noise, mostly caused by patients muscle contractions during recording, from the ECG signals a 10 point moving average (low pass) filter (Figure 3.7) which passes low frequencies but attenuates high frequencies chosen and the signals are filtered by using matlab filter function.

*B=(1/10)*ones(1,10) A=1;*

ECGSignal=filter(B,A,ECGSignal) (3.2)

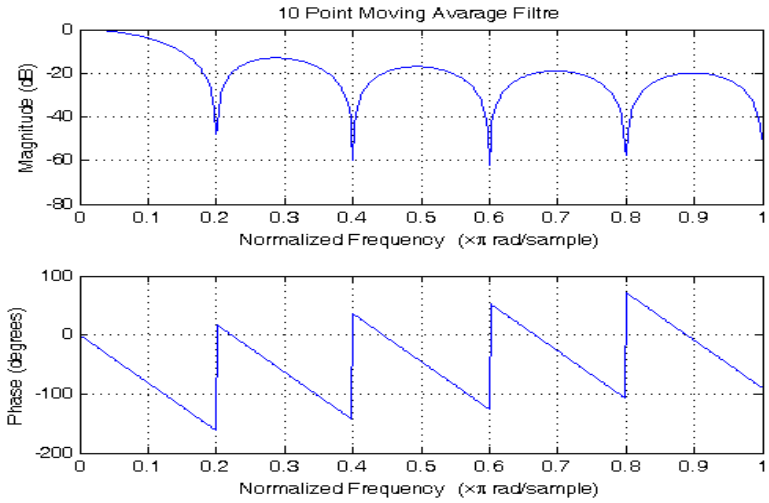

Figure 3.7: Low Pass Filter

After the removal of high frequency noise from the signal next step is to remove low frequency noise components. This low frequency noise shows itself as baseline wandering that is caused mostly by the respiration of the patient. To remove this low frequency noise, a derivative based (high pass) filter (Figure 3.8) that passes high frequencies but attenuates low frequencies used.

B=(1/1.0025)[1 -1];*

A=[1 -0.995];

ECGSignal=filter(B,A,ECGSignal) (3.3)

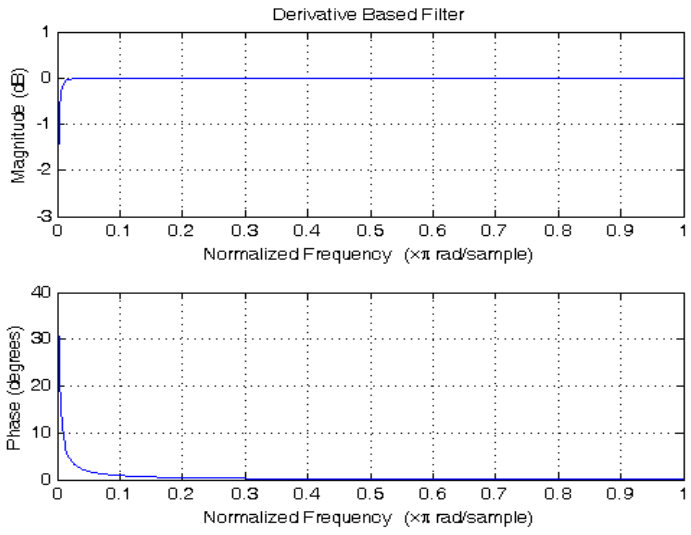

Figure 3.8: High Pass Filter

3.4.3 Removing 60Hz Power Line Interference

Power line interference is a noise caused by the electricity current flowing in wires and power lines. Power line interference that is present in our ECG signals consists of 60Hz pickup and harmonics. Since frequency of 60Hz overlaps with our ECG signal frequency range we have to suppress only 60Hz frequency components and its harmonics without disturbing the frequencies around. To achieve this, comb filter (Figure 3.9) is used and 60Hz power line interference with its harmonics is removed from the ECG signals. Comb filter is a band-stop filter which attenuates a certain band of frequencies and their harmonics.

B=conv([1 1],[0.6310 -0.2149 0.1512 -0.1288 0.1227 -0.1288 0.1512 -0.2149 0.6310]);

A=1;

ECGSignal=filter (B,A,ECGSignal) (3.4)

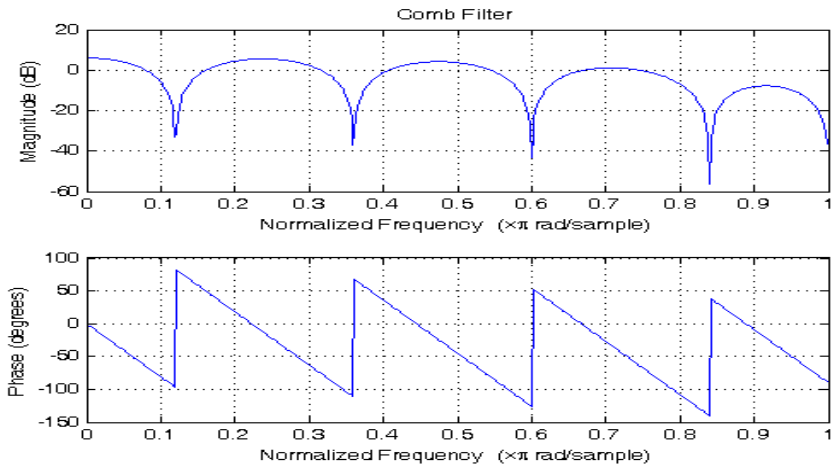

Figure 3.9 Comb. Filter

All of the above steps are applied to all training and testing ECG record and filtered ECG signals (Figure 4.0.) are obtained ready for the next QRS detection step.

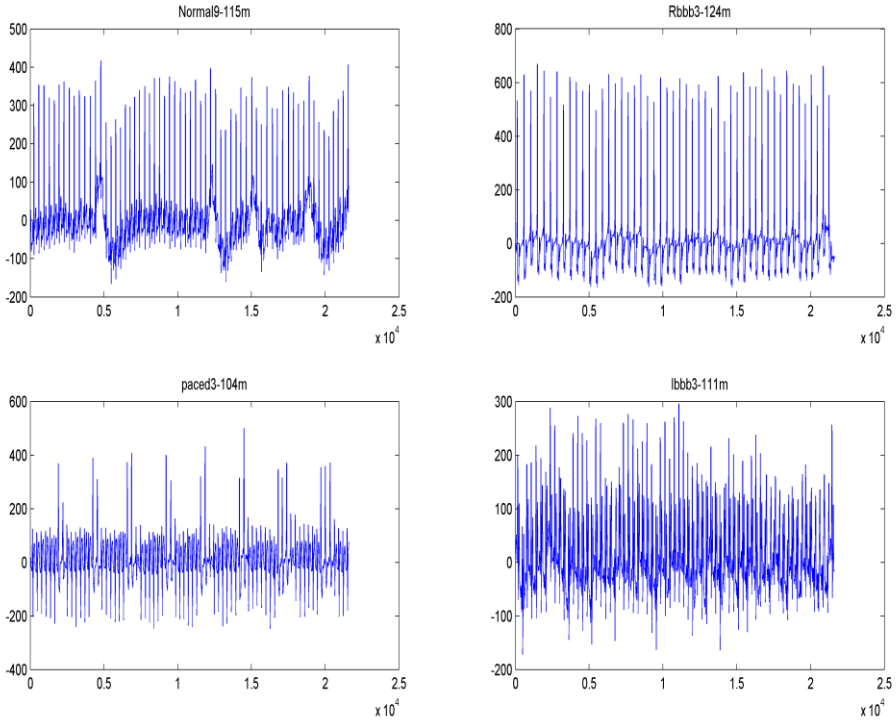

Figure 4.0: Sample filtered ECG signal after preprocessing

3.5 QRS Detection

As mentioned before in previous chapter, the QRS complex is the most striking waveform within the ECG. Since it reflects the electrical activity within the heart during the ventricular contraction, the time of its occurrence as well as its shape provide much information about the current state of the heart. Due to its characteristic shape it serves as an entry point for classification scheme of cardiac cycle. In that sense, QRS detection provides the fundamentals for almost all automated ECG analysis algorithm. To supporting this, previous researchers (Ozbay Y. And Karlik B., 2001) proved that taking samples as feature values in the intervals of R-R are very effective in representing the class of those ECG waves (one cardiac cycle) cardiac condition. Apart from this, since the 5 ECG class records, each representing a different cardiac condition, used for training and testing in this thesis are 1 minute long (each containing 60-90 ECG waveform), in order to separate each waveform (we need to do this because cardiologist classify cardiac conditions by looking at single ECG waveforms (cardiac cycles), not by looking at whole record) and

find how many waveforms each record contain, therefore, we also need to detect the QRS complexes.

There are many different QRS detection techniques but this thesis is focused on well known and acceptable QRS detection using Pan-Tompkins algorithm (Pan J and Tompkins WJ., 1985). Pan and Tompkins proposed a real-time QRS detection algorithm based on analysis of the slope, amplitude and width of QRS complexes. The algorithm includes a series of methods that perform derivative, squaring, integration, adaptive threshold and search procedures.

3.5.1 Derivative Operator

The derivative procedure suppresses the low-frequency components of the P and T waves, and provides a large gain to the high-frequency components arising from the high slopes of the QRS complex. Derivative operation is implemented in Matlab by using *diff* function which finds the differences between the adjacent values in the signal.

$$Derivative=diff(ECGSignal) \quad (3.5)$$

3.5.2 Squaring Operation

The squaring operation makes the result positive and emphasizes large differences resulting from QRS complexes; the small differences arising from P and T waves are suppressed. QRS complex is further enhanced. Squaring operation is implemented simply by multiplying the signal by itself in Matlab.

$$Squaring=derivative.*derivative \quad (3.6)$$

3.5.3 Integration

The output of a derivative based operation may contain multiple peaks within the duration of a single QRS complex. A moving window integrator is applied to perform smoothing of the output of the preceding operations so that multiple peaks are avoided. This step is performed in Matlab by using medfilt1 function and a window width of 54 is found to be suitable for sampling frequency 360Hz.

Window = ones[1,54]; Integration=
medfilt1(filter(window,1,squaring),10); (3.7)

3.5.4 Thresholding

Maximum value of the signal that had passed from above steps is taken and multiplied by a threshold percentage value. This is done because the output of preceding operations may contain noise peaks. These noise peaks do not have as large amplitude as R peaks but if we take all the peaks present in the output of above steps as R peaks then noise peaks will also be classified as R peaks (QRS complexes). So by taking a certain percentage of the highest peak amplitude as a threshold we avoid this. Different values for threshold percentage were tested and value 0.2 found to be suitable for removing noise peaks in our signals. This threshold value is used for searching R peak in search procedures.

Maxvalue = max (integration)
*threshold=maxvalue*0.2* *(3.8)*

3.5.5 Search Procedures for QRS (Location of R Peaks)

In the last step of QRS detection, regions of the output signal, of the preceding steps, that is above the threshold value is found. Starting and ending locations of each region is recorded. Then each specific region is again searched on the original ECG signal for a maximum value which represents the exact R peak of that wave. Locations of all R peaks are then recorded and the QRS searching algorithm is finalized (Figure 4.1).

position_region=integration>threshold
left=find(diff([0 position_region])==1)
right=find(diff([position_region 0])==-1)
for i=1:length(left)
[maxvalue(i) maxlocation(i)]=max(ECGSignal(left(i):right(i)))

end

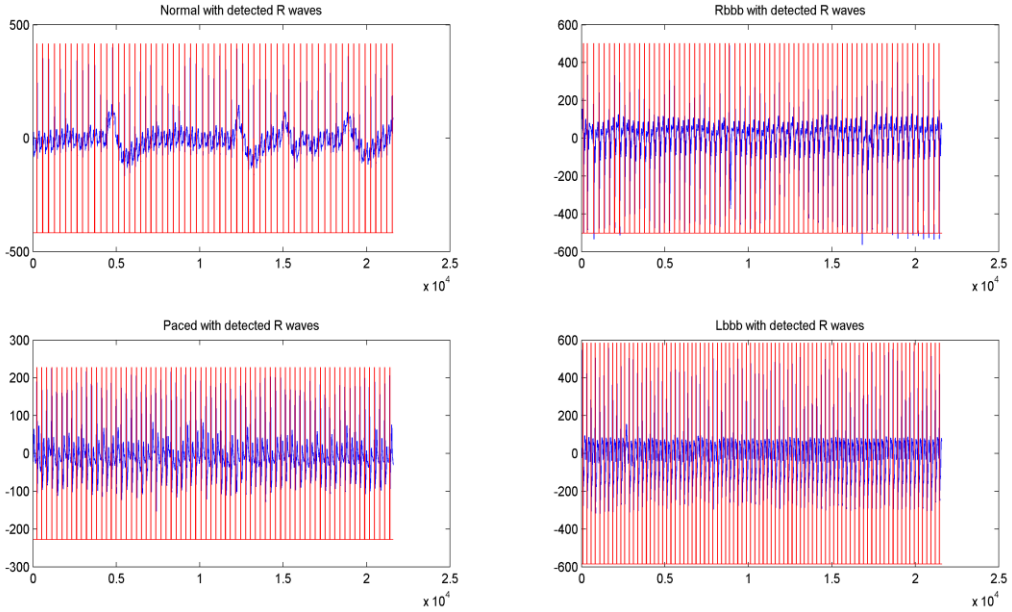

Figure 4.1: ECG signal with R peaks detected

CHAPTER 4

HIGHER ORDER SPECTRA TECHNIQUES

4.1 Introduction

Higher order spectra (HOS) techniques were first applied to real signal processing problems in 1970s, and since then they have continued to expand into different fields such as plasma physics, optics, speech and biomedicine. The estimation of power spectrum of discrete-time deterministic or stochastic signals is one of the most fundamental and useful tools in digital signal processing. The use of power spectrum spreads across radar, sonar, communications, speech, biomedical, geophysical and other data processing systems. In power spectral estimation, the signal under consideration is processed in such a way that the distribution of power among its frequency components is estimated. As such, phase relations between frequency components are suppressed. The information contained in the power spectrum is essentially that which is present in the autocorrelation sequence; and is sufficient to describe a Gaussian signal completely. HOS offers some unique features that make it more advantageous for use in some applications. Some of the motivations behind the use of higher order spectra in signal processing are as in (Chua.2010) are as follows:

i. HOS of non-Gaussian linear processes contains both amplitude and phase information. They have been used for time-series modeling, and identification of non-minimum phase and non causal systems. These applications include signal reconstruction from speckle images, seismic de-convolution and channel equalization.

ii. The HOS of Gaussian signal is statistically zero. Thus, HOS can be used to measure non-Gaussianity and to separate additive mixtures of independent non-Gaussian signal and Gaussian noise. This feature can be exploited to detect

and classify non Gaussian signals and provide high noise immunity in application where the signal source is corrupted with Gaussian noise.

iii. A general non-linear system can be modeled using Nth-order Volterra processor (Schetza, 1980). HOS is able to detect and characterized the non-linear properties of mechanism which generate time-series via phase relations of their harmonic components.

iv. HOS are translation invariant because linear phase terms are cancelled in the products of Fourier coefficient that define them. Functions that can serve as feature for pattern recognition can be defined from higher order spectra that satisfy other desirable invariance properties such as scaling, amplification and rotation invariance.

4 .2 Higher Order Spectra

Higher order spectra are defined to be spectral representation of higher order cumulants of a random process.

In this section, we introduce the definitions, some properties and computation of higher-order statistics, i.e., moments and cumulants, and their corresponding higher-order spectra.

4.2.1 Moments

A random variable is a quantity whose values are random and to which a probability distribution is assigned. Formally, a random variable is measurable function from a sample space to the measurable space of possible values of the variable.

As the term implies, the moment generating function should be able to generate all moments. For any random variable x, the moment generating function can be defined as the expectation of the transformation, e^{tx} where $\mathrm{t} \in R\ i.e$

$$Mx(t) = e^{tx} \tag{4.1}$$

Moments can be obtained from the coefficients of the Taylor's series expansion of the moment generating function about the origin, t=0

$\mathrm{Mx(t)} = Mx(t) + \frac{\partial Mx(t)}{\partial t}(t-0) + \frac{1}{2!}\frac{\partial Mx(t)}{(\partial t^2)}\ (\mathrm{t}-0)^2 + \frac{1}{3!}\frac{\partial Mx(t)}{(\partial t^3)}(\mathrm{t}-0)^3 + \cdots,$

=

$$\mathrm{Mx(t)} = Mx(t) + \frac{\partial Mx(t)}{\partial t}(t) + \frac{1}{2!}\frac{\partial Mx(t)}{(\partial t^2)}\mathrm{t}^2 + \frac{1}{3!}\frac{\partial Mx(t)}{(\partial t^3)}t^3 + \cdots, \qquad (4.2)$$

From the right hand side of equation 4.2, the first derivative gives the first order moment ;

$$M1 = \frac{\partial Mx(t)}{\partial t}$$

Substituting the $Mx(t) = E^{tx}$

$$\mathrm{M1} = \frac{\partial [E^{tx}]}{\partial t} = E(xe^{tx}) = E[x] \qquad (4.3)$$

Where E is expected operator

The second derivative gives the second-order moment

$$\mathrm{M2} = \frac{\partial^2 Mx(t)}{\partial \mathrm{t}^2} = \frac{\partial^2 [E^{tx}]}{\partial \mathrm{t}^2} = E(x^2e^{tx}) = E[x^2] \qquad (4.4)$$

Similarly, the derivative of the third order moment is

$$\mathrm{M3} = E[x^3] \qquad (4.5)$$

And so on. Therefore we can write the moment generating function as

$Mx(t) = E^{tx}$ =E$[1 + tx + \frac{t^2}{2!}x^2 + \frac{t^3}{3!}x^3 + \cdots,]$

=1+t$E[x] + \frac{t^2}{2!}E[x^2] + \frac{t^3}{3!}[\![E[x]]\!]^3] + \cdots$

$$=1+tM1+\frac{t^2}{2!}\mathrm{M2}+\frac{t^3}{3!}\mathrm{M3} \quad (4.6)$$

The first order moment is the mean ($\mu = E(x)$) of the data series, x(k), which provides a measure of the location or the center of gravity of the probability density function (PDF) for an ergodic signal. The second order moment is the variance of the data series and gives the spread of the PDF, while the third-order moment provides a measure of the skewness of the distribution and the fourth-order moment provide a measure of the flatness of the distribution.

4.2.2 Cumulants

These are another set of statistical measure that can be used instead of moments because of their excellent noise suppressing properties. The cumulant generating function is defined as the logarithm of the moment generating function. That is for a random variable x the cumulant generating function is

$$Cx(t) \triangleq \ln Mx(t) \quad (4.7)$$

Just as moments are derived from the Taylor's series expansion of the moment generating function, cumulant can also be derived. But one can easily calculate cumulants as certain nonlinear combination of moments. The second, third and fourth-order cumulants are given (Nikias et al, 1993b).

$$C_1{}^x = M_1{}^x$$

$$C_2{}^x(\tau) = M_2{}^x(\tau) - (M_1{}^x)^2.$$

$$C_3{}^x(\tau_{1,}\tau_{2,}) = M_3{}^x(\tau_{1,}\tau_{2,}) - M_1{}^x[M_2{}^x(\tau_1) + M_2{}^x(\tau_2) + M_2{}^x(\tau_2 - \tau_1) + 2(M_1{}^x)^3$$

$$C_4{}^x(\tau_{1,}\tau_{2,}\tau_3) = M_4{}^x(\tau_{1,}\tau_{2,}\tau_3) - M_2{}^x(\tau_1)\, M_2{}^x(\tau_3 - \tau_2)$$

$$-M_2{}^x(\tau_2)M_2{}^x(\tau_3 - \tau_1) - M_2{}^x(\tau_3)M_2{}^x(\tau_2 - \tau_1)$$

$$-M_1{}^x[M_3{}^x(\tau_2-\tau_1,\tau_3-\tau_1)+\ M_3{}^x(\tau_2,\tau_3)+M_3{}^x(\tau_1,\tau_2)]$$

$$+(M_1{}^x)^2[M_2{}^x(\tau_1)+M_2{}^x(\tau_2)+M_2{}^x(\tau_3)+M_2{}^x(\tau_3-\tau_1)$$

$$M_2{}^x(\tau_3-\tau_2)M_2{}^x(\tau_2-\tau_1)]-6((M_1{}^x)^4. \quad (4.8)$$

If the signal x(k) is zero mean then the second and third-order cumulants are identical to second and third order moments respectively. If the process has non- zero mean, then the mean may be subtracted from its self and this is often the practice with estimation from finite records. However, to generate the fourth-order cumulant we need to have the knowledge of the fourth-order and second-order moments. i.e

$$C_4{}^x(\tau_{1,}\tau_{2,}\tau_3)=M_4{}^x(\tau_{1,}\tau_{2,}\tau_3)-M_2{}^x(\tau_1)\ M_2{}^x(\tau_3-\tau_2)$$

$$-M_2{}^x(\tau_2)M_2{}^x(\tau_3-\tau_1)-M_2{}^x(\tau_3)M_2{}^x(\tau_2-\tau_1) \quad (4.9)$$

In practice, because of the unique linear property of the second characteristic function working with cumulants and cumulant spectra instead of moments is more common and preferable in the case of stochastic signals.

However, it is noteworthy that estimates of cumulants are obtained in practice after computing estimates of moment from time domain samples using their relationship. Besides, higher order spectra are often estimated directly in the spectral domain as expected values of higher order period gram. In cases where HOS are estimated in spectral domain, cumulants may not be calculated. Cumulant spectra can be obtained from moment spectra in the spectral domain through similar relationships (Billinger et al, 1967; Nikias et al, 1987; Chandran et al, 1994).

Cumulants of the first three orders at zero lag are the well known parameters, variance, skewness and kurtosis used to describe probability density functions.

By putting $\tau_{1=}\tau_{2=}\tau_3$ into the equations above, we obtain;

$$\gamma_2{}^x=E\{(x_2)\}=C_2{}^x(0) \quad \text{(variance)} \quad (4.10)$$

$$\gamma_3{}^x = E\{(x_2)\} = C_3{}^x(0,0) \quad \text{(skewness)} \tag{4.11}$$

$$\gamma_4{}^x = E\{(x_2)\} - 3[\gamma_3{}^x]^2 = C_4{}^x(0,0,0) \quad \text{(kurtosis)} \tag{4.12}$$

The above three equations gives the variance, skewness and kurtosis measures in terms of cumulants at zero lags.

Some of the properties of cumulants that any nth-order cumulants satisfy are

i. Cumulants of scaled quantities are equal to the product of all the scale factors times the cumulants of the unscaled quantities.
ii. Cumulants are symmetric in their arguments. i.e
iii. Cumulants are additive in their arguments i.e. cumulants of sums of cumulant
iv. Cumulants are blind to additive constant

4.2.3 Bispectrum

The method used for estimating the second-order spectrum or power spectrum can easily be extended to obtaining frequency domain counterparts of higher order cumulants. Hence the bispectrum is the frequency domain representation of the third-order cumulant. It ıs defined as

$$B(f1, f2) \triangleq \text{DDFT}\left[f(x) = [c_3(\tau_1, \tau_2)]\right] = [\text{x(f1)x(f2)} * (\text{f1} + \text{f2})] \tag{4.13}$$

The above equation shows that the bispectrum is a complex quantity having both magnitude and phase. It can be plotted against two independent frequency variables f1 and f2, in a three dimensional plot.

4.2.4 Bicoherence

The bispectral estimates of bispectrum are asymptotically unbiased and the variance of the estimator depends on the second-order spectral properties (Hinich et.al, 1982).

Since the estimates depends on signal energies in the bifrequency, the variance of the estimate will be higher at a frequency where the energy is high and

lower where the energy is low. This causes a serious problem in the estimation. This unsatisfactory property can be resolved in so many ways. One of which is the normalization. Hence, bicoherence is the normalization of the bispectrum to get a new measure whose variance is independent of the signal energy.

4.3 Estimation of Higher Order Spectra

In practice, even if the underlying process is random and continuous, digital computations require discrete or sampled data and the data available are of finite length. Just like the power spectra, there are two main approaches that can be used to estimate higher order spectra (Nikias et al, 1993b): the conventional non-parametric method (or "Fourier type") and the parametric approach. In this research we use the non-parametric approach. In this approach, the Matlab based higher order spectral analysis tool box (HOSA) which consist of various functions to estimate HOS both in parametric and non-parametric methods, as well as some utility functions for various test and measurement was used for computing both the amplitude and their corresponding frequencies.

The main estimation parameters that need to be chosen for bispectral analysis are the same parameters as required for second-order spectral analysis. Examples include the choice of window function, data length, data segment length, length of Fourier transform, and overlapping or non-overlapping windows (Fackrell, 1996). The above mention parameters were chosen as follows;

Choice of window function: In spectral analysis, the use of a window function is very common. The main reason for using a window is to solve the problem of spectral leakage that occurs between neighboring frequencies channels of a peak. Spectral leakage is the term used to describe the loss of power at a given frequency to other frequency bins in the DFT. Spectral leakage can be visualized from the spread of the frequency components. Each frequency component of a signal should contribute only to one single frequency of the

Fourier transform called a FFT bin, but spectral leakage causes the energy to be spread to the neighboring frequencies. The window function controls the spreading. The contribution from any real frequency component to a given FFT bin is weighted by the amplitude of the window function's frequency spectrum centered at the FFT bin.

The performances of three window functions have been compared in Fackrell (1996) and it has been shown that the Hamming window was the most successful among them to best resolve the peak. The Hanning window
Stand next to the Hamming window in terms of peak resolution. Hence we choose the Hanning window because it is the default window in the HOSA tool box.

Choice of data length and segment length: It is well known that bispectral estimates generally have higher variance than power spectral estimates for a given data length. The data length that is sufficient for reliable power spectrum estimation may not be sufficient for good bispectral estimation. Elgar and Guza (1988) reported empirical results for mean and variance of bicoherence estimates. Hinich (1982) suggested that if no frequency domain smoothing is used, the data should be segmented in a way such that the number of segments of data should be at least as large as the DFT size, i.e. $K \geq M$. However, this may not be achievable and therefore it may be impractical to implement bicoherence in real-life applications. The bottom line is that the number of data segments used in the bicoherence should be sufficient to have asymptotically unbiased and consistent estimation as well as to keep a good frequency resolution. In practical bispectral analysis, the length of data required depends on signal-to-noise ratio.

Choice of Fourier transform length: In choosing the Fourier transform length, we need to consider how the bicoherence peak changes with SNR and segment length. When the SNR is very high, the bicoherence will be close to unity, but when it decreases, the bicoherence value also decreases. The size of the peak of the bicoherence is dependent on the segment length, because as the

FFT size increases a better frequency resolution is obtained. Therefore it is desirable to have the FFT as large as possible. However, this requirement conflicts with the requirement of having a large number of data segments, to obtain reliable estimate. It also increases the computational load as shown in figure 4.1 and 4.2 below .The FFT length is usually chosen to be the same as each segment length. In order to increase the number of data segment for a better estimate, a certain amount of overlapping of data segments (e.g 50% or less) can be allowed for data sets having short length.

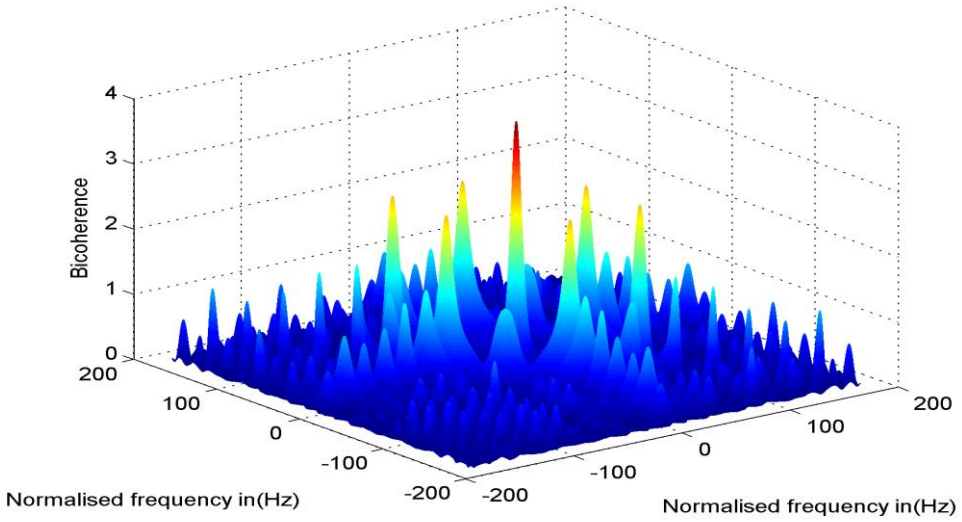

Figure 4.1 3-D bicoherence plot with an FFT of 2048

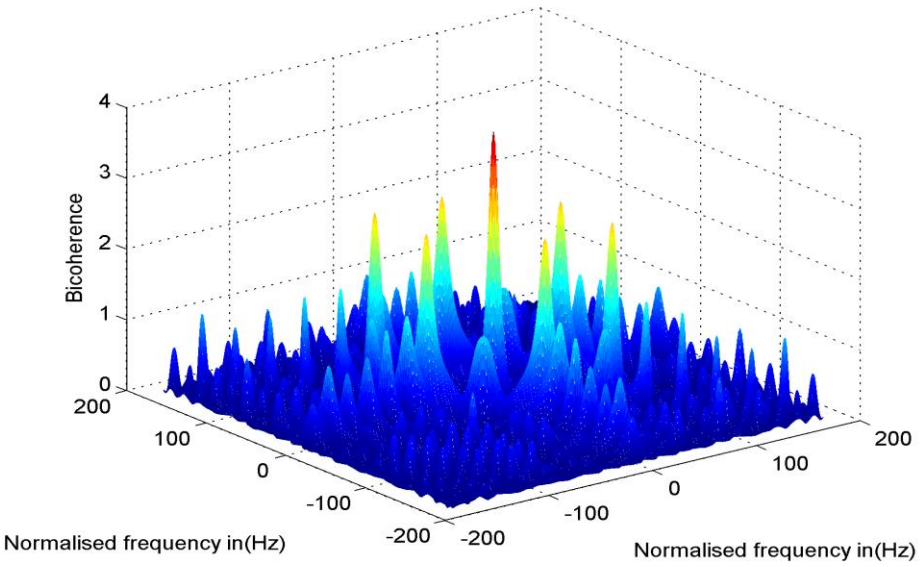

Figure 4.2 3-D bicoherence plot with an FFT of 512

4.5 Statistical Variables

In this thesis, the higher order statistical parameters used as features are the skewness, kurtosis and variance. A brief explanation of each one of them is given below:

Skewness: is the third mean and is a measure of the asymmetry of the processes. For symmetric distribution skewness is identically zero.

Kurtosis: is the fourth moment about the mean and is related to the degree of flatness of a distribution near its center. For Gaussian distribution, the value of kurtosis is 3. The values of more than 3 are indicating that the probability density function (PDF) is more peaked around its center than a Gaussian distribution.

Variance: is the measure of the spread of the data from the mean.

4.6 Classifiers

4.6.1 Artificial Neural Network

One of the classifiers used in this analysis is the artificial neural network (ANN), which is biologically inspired network that are useful in application areas such as pattern recognition, classification etc. The decision making process of the ANN is holistic, based on the features of input patterns. Typically, multilayer feed forward neural network can be trained as non-linear classifier using generalized back propagation algorithm (BPA) (Haykin et,al. 1995). The BPA is a supervised learning algorithm, in which a mean square error function is defined, and the learning process aims to reduce the overall system error to a minimum. The connection weights are randomly assigned at the beginning and progressively modified to reduce the overall system error. The weight updating starts with the output layer and progressing backward.

For effective training, it is desirable that the training data set be uniformly spread throughout the class domains. The available data can be used iteratively, until the error function is reduced to a minimum.

The ANN used for classification in this work is shown in Fig. 4.6. The input layer is determined based on the features used at a particular classification, but we fixed the hidden layer at 20 for the training and testing of all features with an output layer of 5. i.e from [1 0 0 0 0] to [0 0 0 0 1]. The advantage of the ANN classifier using the proposed features is its simplicity and ease of implementation.

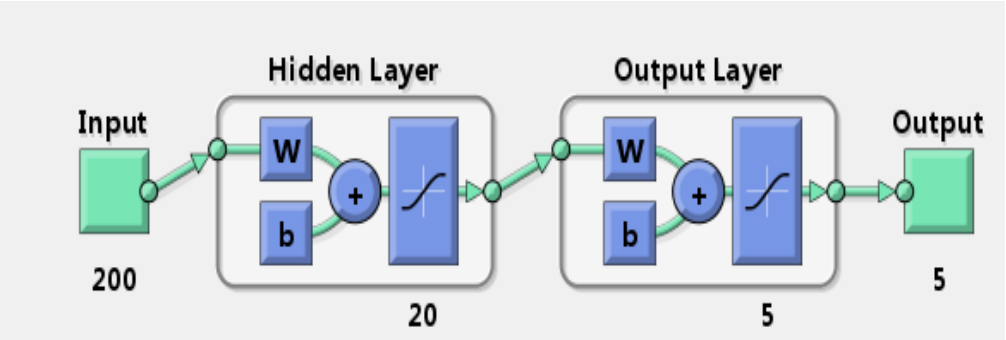

Fig.4.3 The feedforward neural network

4.6.2 K-Nearest Neighborhood Search

The knn search technique and knn-based algorithm are widely used as benchmark learning rules. The relative simplicity of the knn search technique makes it easy to compare the results from other classification to knn result. They have been used in various areas such as bioinformatics, image processing and compression among others. Given a set of data X of n points and a distance function D, k-nearest neighborhood (KNN) search allows you to find the k closest points in X to a query point or set of points.

But one of the problem with machine learning is the 'curse for high dimensionality' when there are too many attributes in the input as in this case, many of the machine learning algorithm will be very inefficient or some of them will be even non performing. Principal component analysis is a technique that can be used to solve this problem without much loss of information in the data. PCA selects the attribute that are later dependent on each other and from them a smaller subset of independent variable may be derived and still be very useful to describe the data characteristics.

Given a set described by a set of numerical variables $\{x_1, x_2, x_3 \dots \dots \dots x_n\}$, the goal of principal component analysis is to describe this data set with a smaller set of new, synthetic variables. These variables will be linear combinations of the original variables, and are called PCA. PCA will lead to some loss of information. However, PCA operates in a way that makes this loss minimal.

The steps of PCA are as follows:

1. For a given input data $x = \{x_1, x_2, x_3 \dots \dots \dots x_n\}^T$, obtain the mean of the data. $\mu_x = E\{x\}$.
2. Compute the covariance matrix; $C_x = \mathrm{E}\{(x - \mu_x)(x - \mu_x)\}^T$.
3. From the covariance matrix, the eigenvectors and eigenvalues are being calculated using the characteristics equation; $\det(C_x - \alpha I) = 0$
4. Project the data to the lower dimension subspace by taking the dot product between the given data and principal component (PCs) from the eigenvectors.

CHAPTER 5

RESULTS AND DISCUSSION

5.0 Method

The ECG signal was analyzed using different higher order spectra (also known as polyspectra) that are spectral representation of higher order moments or cumulants of a signal. In particular, this work studied the features related to the third order statistics of the signal, namely the bispectrum and bicoherence (normalized bispectrum), and then the skewness, kurtosis and variance related to these higher order statistics were computed.

The methods employed in this work are as follows:

❖ ***Feature Extraction and Classification for Statistical Parameters***

- The statistical features have been extracted from each R-T interval
- In the normal signal we have 366 samples, in rbbb 373, in paced 357, in lbbb 337 and 296 in Apb.
- The total samples been 1729 was used to find the statistical features
- The higher order statistics parameters of skewness, kurtosis and variance of each sample were also computed and used as features.
- The neural network was fed with 1729x3 for training samples and 640x3 for testing samples.

❖ ***Feature Extraction and Classification for HOS***

- Bispectrum and bicoherence functions are calculated for 5 set of arrhythmias and 5 waveforms of ECG including several beats to obtain plots in higher resolution.
- The cross-section of the bicoherence spectrum is obtained for those 25 waveforms.
- Then the location and magnitudes of 10 most significant peaks are calculated as another set of features with 25x20 samples and fed to the network.

- After observing that the result is not good enough, the number of samples for each disease is increased to 10 which make the size of features to 50x20.
- Principal component analysis was applied to reduce the features to 35x11 for training and 15x11 for testing.
- Knn-search algorithm was used for classification

5.1 Result using Statistical Parameters

We compute the higher order statistics parameters of skewness, kurtosis and variance at each of the 366 samples in normal, 373 Rbbb, 357 Paced, 337 Lbbb and 296 Apb each at the R-T interval to see the effect of the phase information. A total of 1729 x3 features were obtained and fed to the neural network for training and an average accuracy value of 96.6% was obtained for the classification. The neural network was then tested with 640 samples of which 119 are normal, 140 are Rbbb, 144 paced, 131 lbbb and 106 Apb respectively. The tables below show the results of the testing.

Table 5.1 (a) Confusion matrix for testing of statistical features

Signal	Normal	Rbbb	Paced	Lbbb	Apb
Normal	101	0	1	0	0
Rbbb	0	139	0	1	0
Paced	1	1	127	32	6
Lbbb	17	0	16	92	1
Apb	0	0	0	6	99

Table 5.1(b) Table For the correctly and non correctly classified samples

Signal/parameter	TP	FP	TN	FN
Normal	101	18	520	1
Rbbb	140	0	499	1
Paced	127	17	458	39
Lbbb	92	39	475	34
Apb	99	7	528	6

Table. 5.1 (c) Performance matrix for the testing of statistical features

Parameters	Normal	Rbbb	Paced	Lbbb	Apb	**%Ave.**
Sensitivity%	99	99.3	76.5	73	94.3	**88.4**
Specificity%	96.7	100	92	93.3	98.9	**96.2**
Positive pre.%	84.9	100	88.2	70.2	93.4	**87.3**
Accuracy%	97	99.8	91.4	88.6	97.9	**94.9**

As it can be observed from table 5.1 (c), the statistical features gives an acceptable accuracy with relatively low sensitivity of 88.4% and positive prediction value of 87.3%.

5.2 Result using the Peaks of Bicoherence

Two different classifiers are used to classify the peaks of the bicoherence in this section.

First, the bispectrum and bicoherence were computed using HOSA toolbox with the FFT window size of 512, wind size of 1 which is the same size as the

various signals size, segment size of 18 for each of the five signals and 50% overlap which is 256 have been used and the corresponding bicoherence values were computed. The resulting bispectrum magnitude plots for various types of deseases are shown in (figure 5.1(a)-5.5(a)) ,the bicoherence plots are shown in (figure5.1(b)-5.5(b)), the bicoherence selected peaks plot (figure5.1(c)-5.5(c)) and the 3-D plots are shown in (figure5.1(d)-5.5(d)).

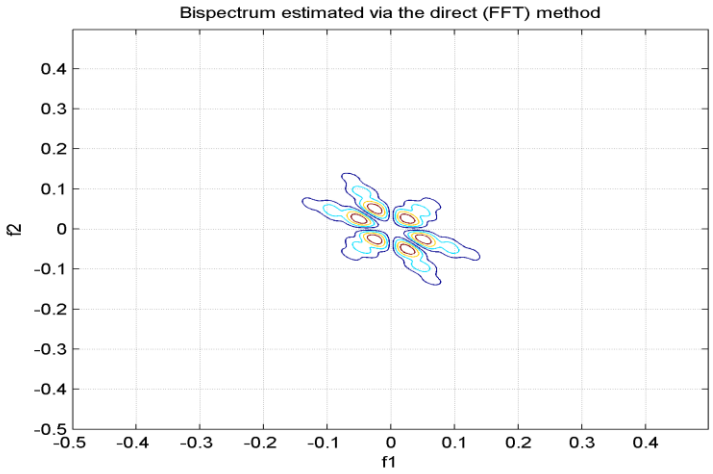

(a)

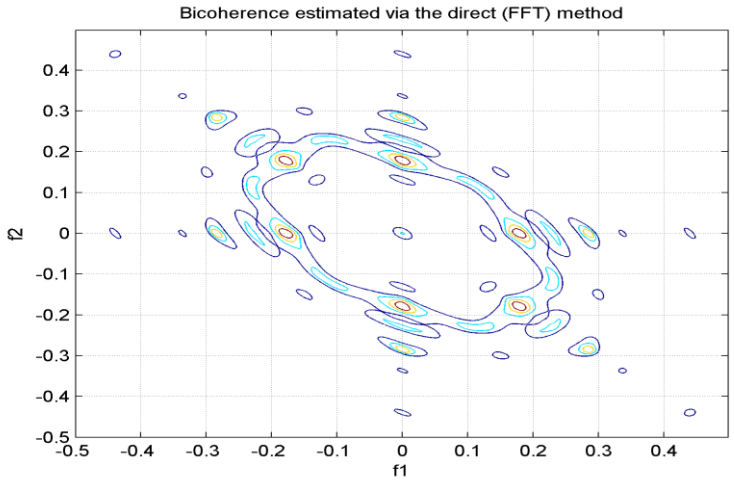

(b)

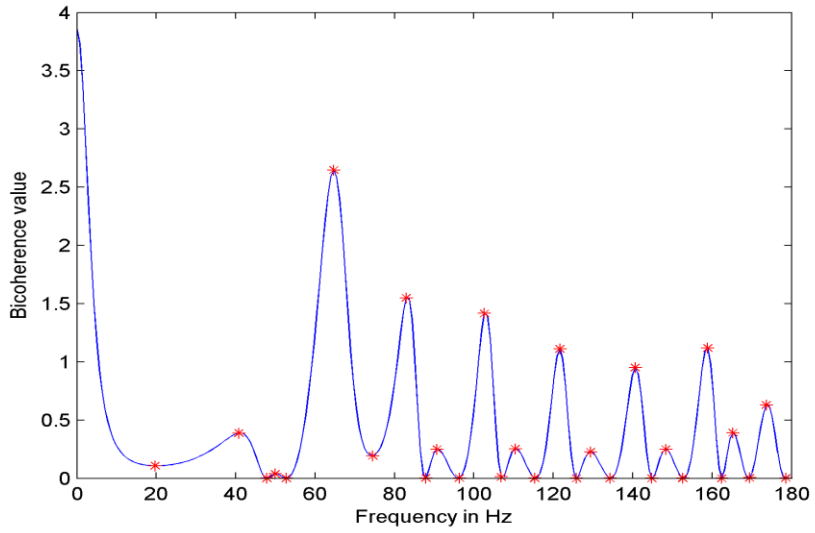

(c)

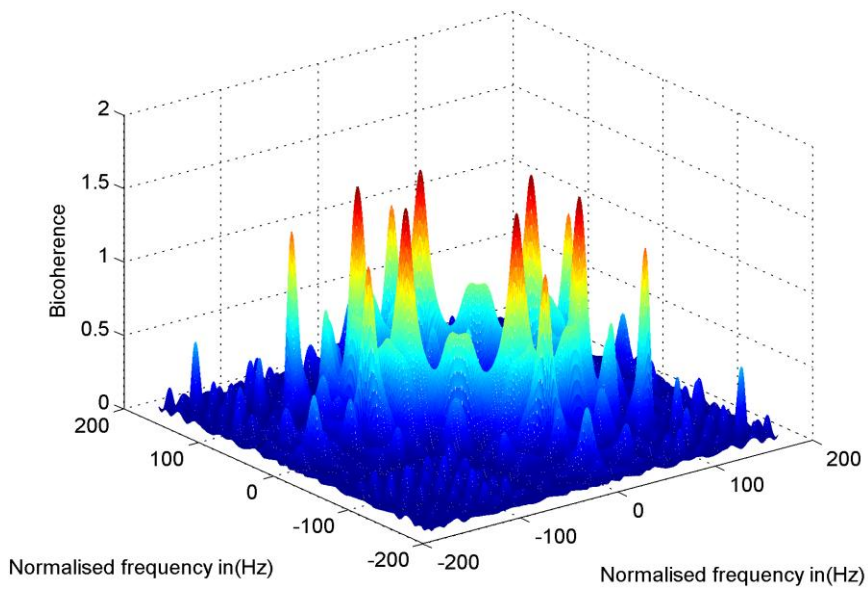

(d)

Figure 5.1 a. Bispectrum, b. Bicoherence c. Bicoherence selected peaks and d.3-D bicoherence plot for normal beat

For the normal cases, the bispectrum magnitude plot exhibit peaks at lower frequencies Fig 5.1(a). The heart rate is varying continuously between 60-80

beats per minute (bpm). The bicoherence values appear to be scattered throughout the bi-frequency plane in a random manner except for a few peaks that are narrow-band. We can observe that the highest peak is at 2.76 with average value of 1.732 as in fig 5.1 (c). It is quite possible that the few peak values are related to the rate of breathing pattern. The fact that these peaks appear in the same vicinity in the number of the other plots supported this argument. However, it can only be verified if there is a corresponding data on respiration. If this happened to be true, any nonlinearity in the data from the nature of the disease must be considered in comparison with effect of this nonlinearity.

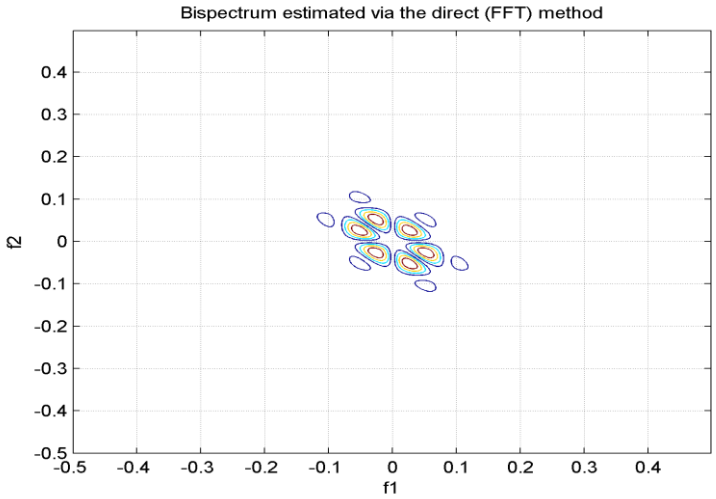

(a)

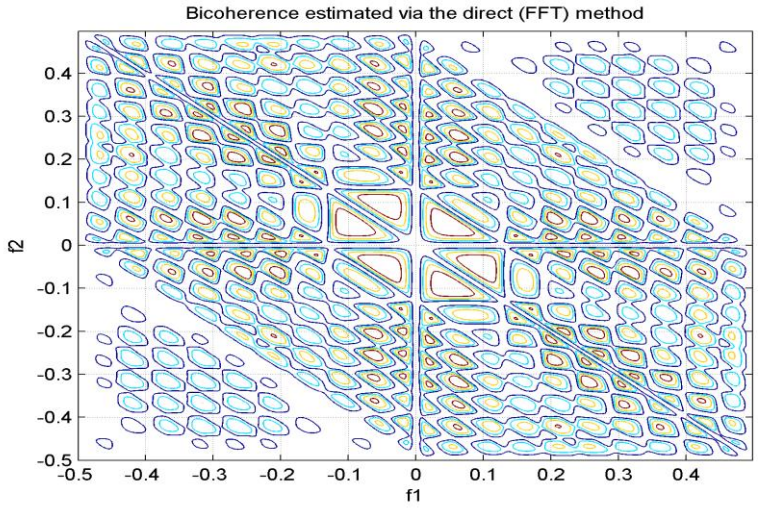
Bicoherence estimated via the direct (FFT) method
f2
f1
0.4
0.3
0.2
0.1
0
-0.1
-0.2
-0.3
-0.4
-0.5
-0.5
-0.4
-0.3
-0.2
-0.1
0
0.1
0.2
0.3
0.4

(b)

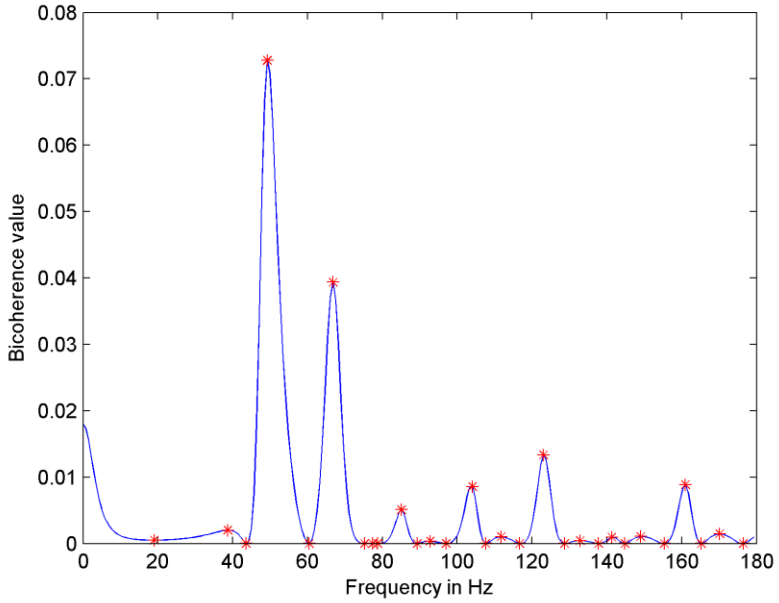
Bicoherence value
Frequency in Hz
0.08
0.07
0.06
0.05
0.04
0.03
0.02
0.01
0
0
20
40
60
80
100
120
140
160
180

(c)

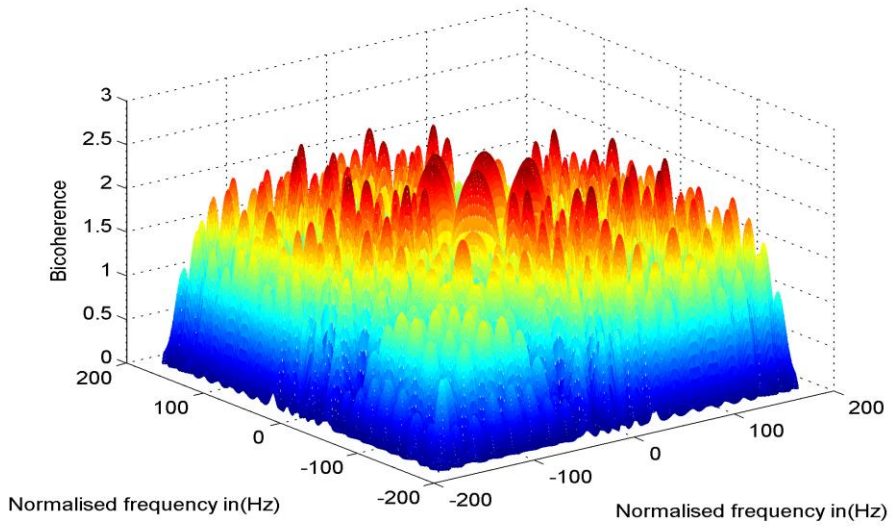

(d)

Figure 5.2 a. Bispectrum, b. Bicoherence c. Bicoherence selected peaks and d.3-D bicoherence plot for rbbb beat

In the case of the Right bundle branch block, most of the peaks in the plots are at high frequency. The bicoherence values appear to be congested at the centre of the bifrequency plane and are more structured compare to normal. Fig 5.2(c) shows clearly how the bicoherence values are located with most of the values at lower level, with the average value been at 2.27.

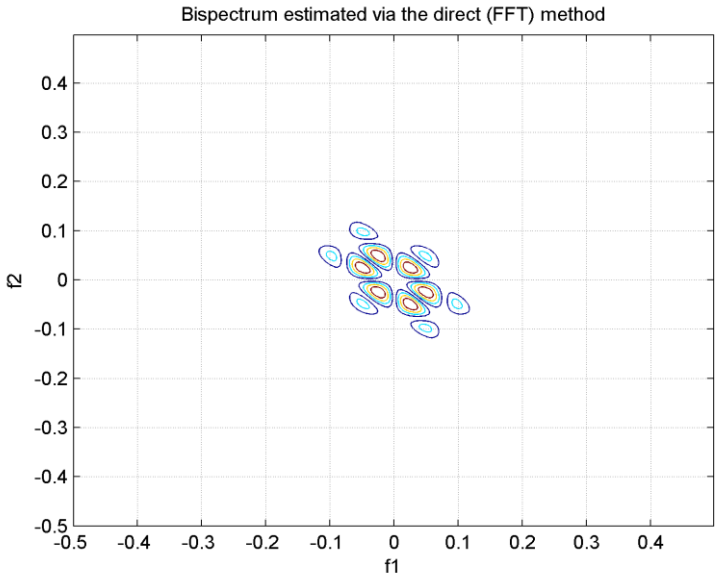
Bispectrum estimated via the direct (FFT) method
f2
f1
0.4
0.3
0.2
0.1
0
-0.1
-0.2
-0.3
-0.4
-0.5
-0.5 -0.4 -0.3 -0.2 -0.1 0 0.1 0.2 0.3 0.4

(a)

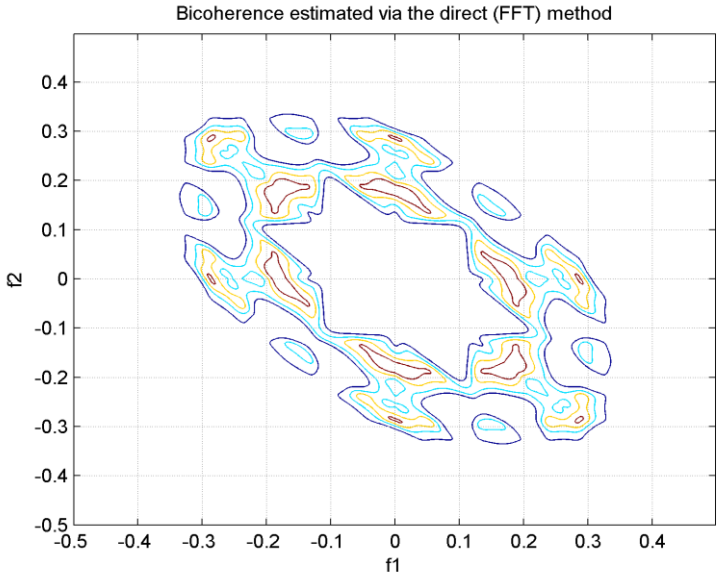
Bicoherence estimated via the direct (FFT) method
f2
f1
0.4
0.3
0.2
0.1
0
-0.1
-0.2
-0.3
-0.4
-0.5
-0.5 -0.4 -0.3 -0.2 -0.1 0 0.1 0.2 0.3 0.4

(b)

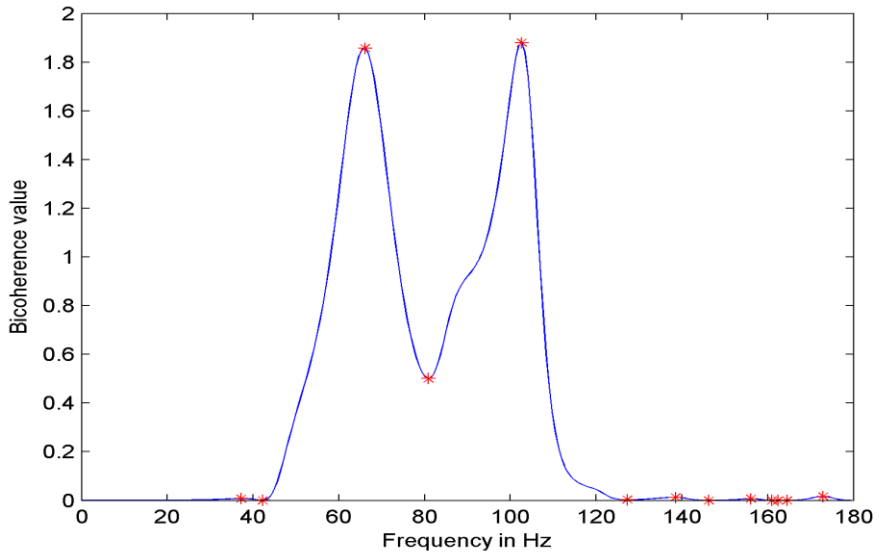

(c)

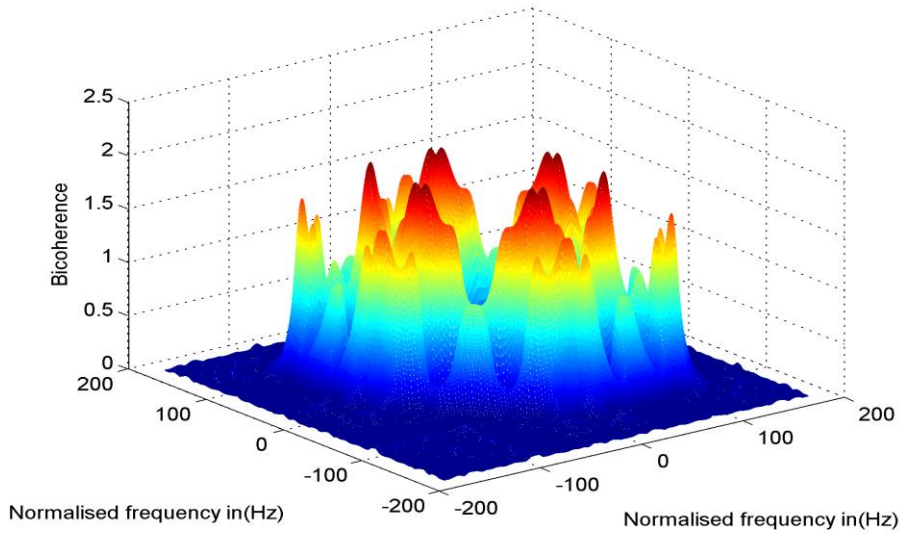

(d)

Figure 5.3 a. Bispectrum, b. Bicoherence c. Bicoherence selected peaks and d.3-D bicoherence plot for Paced beat

In the paced beat, the bispectrum magnitude plot exhibits peaks at low frequency just as in normal beat, because sometimes the A-V node fails to send electrical signals rhythmically to the ventricles, which make the heart rate to remain low and even lead to complete heart block. The bicoherence plot indicates a spreading in the bifrequency plane with more peaks crowded at higher frequencies. Fig 5.3(c) shows how the bicoherence values are distributed, with the average been 1.98.

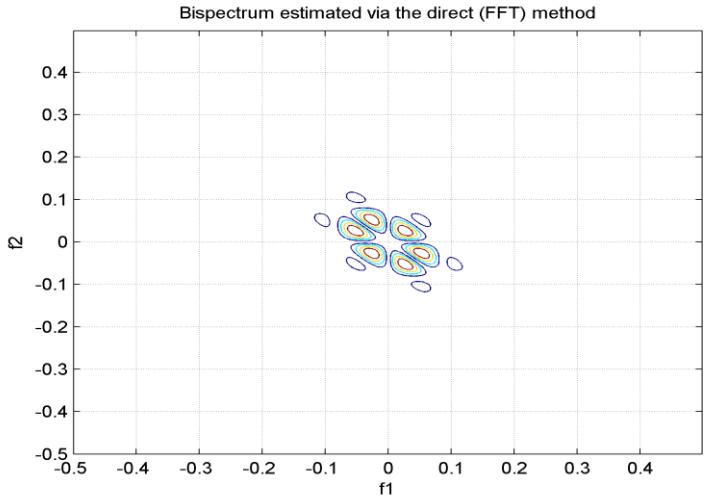

(a)

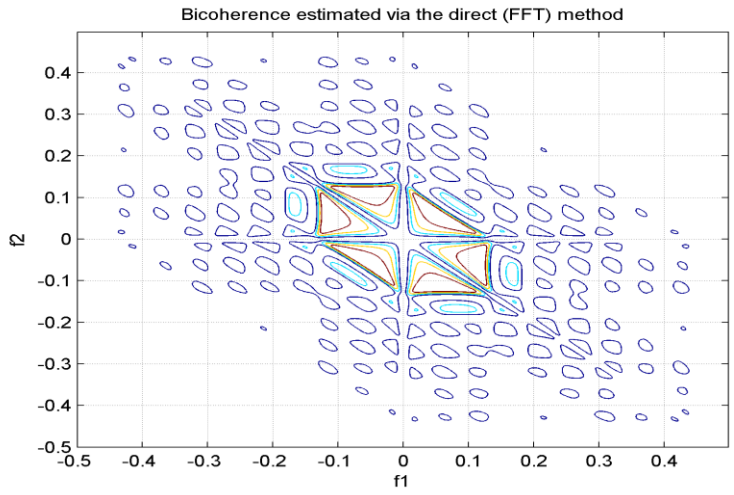

(b)

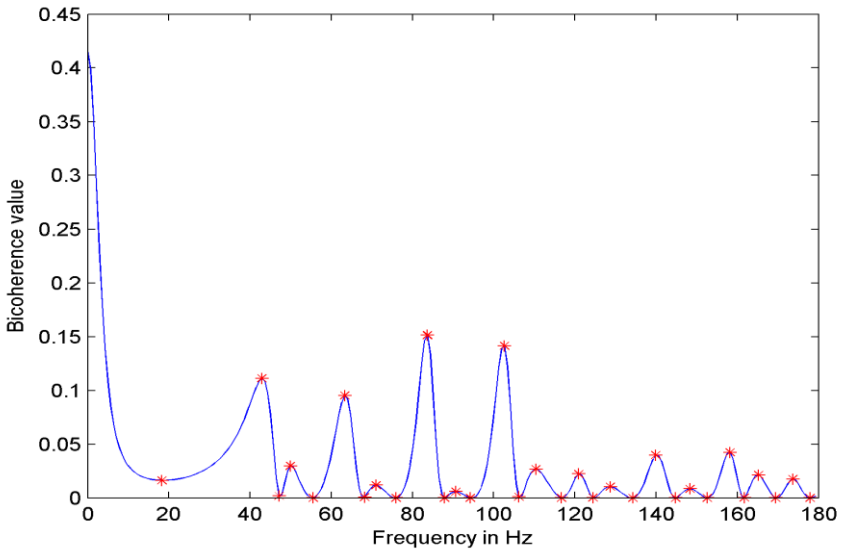

(c)

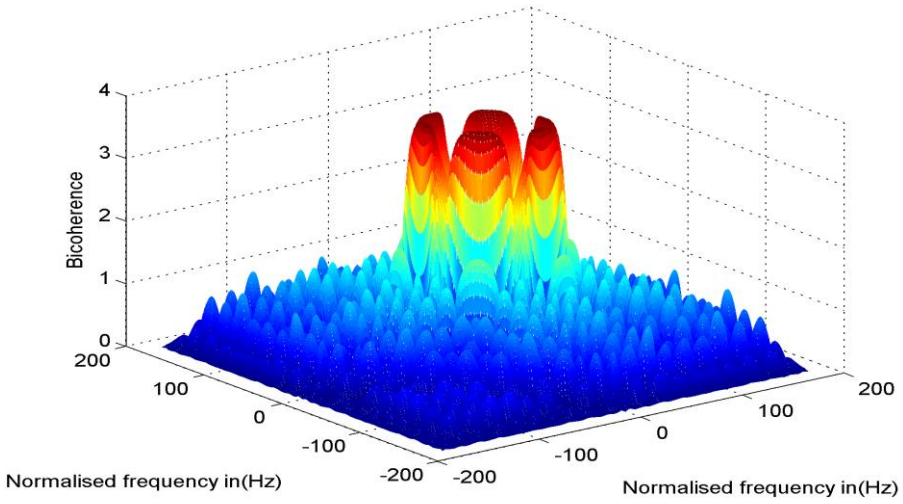

(d)

Figure 5.4 a. Bispectrum, b. Bicoherence c. Bicoherence selected peaks and d.3-D bicoherence plot for lbbb beat

In the case of the left bundle branch block, the bispectrum shows peaks at higher frequencies, since the heart rate variation in Lbbb is high. The bicoherence plot indicates more structure than the normal case. Fig 5.4 (c)

shows that most of the bicoherence values are at higher frequencies, with the average been 2.94.

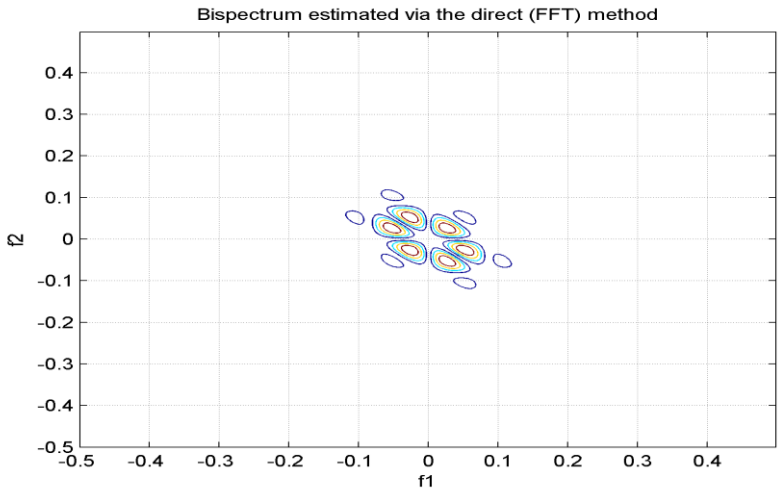

(a)

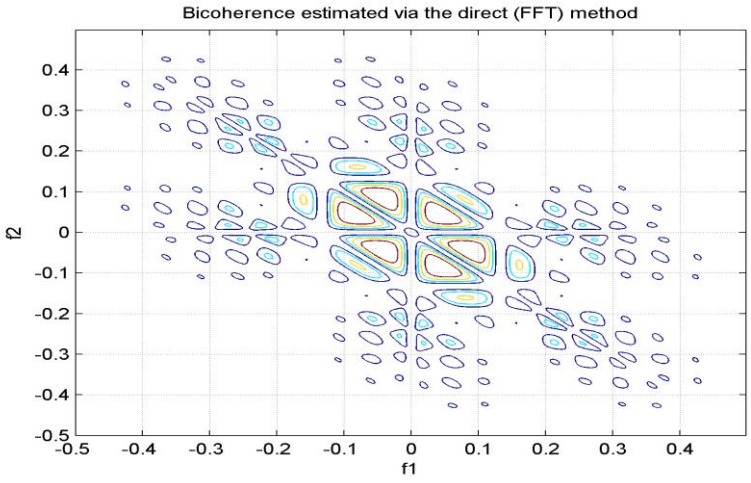

(b)

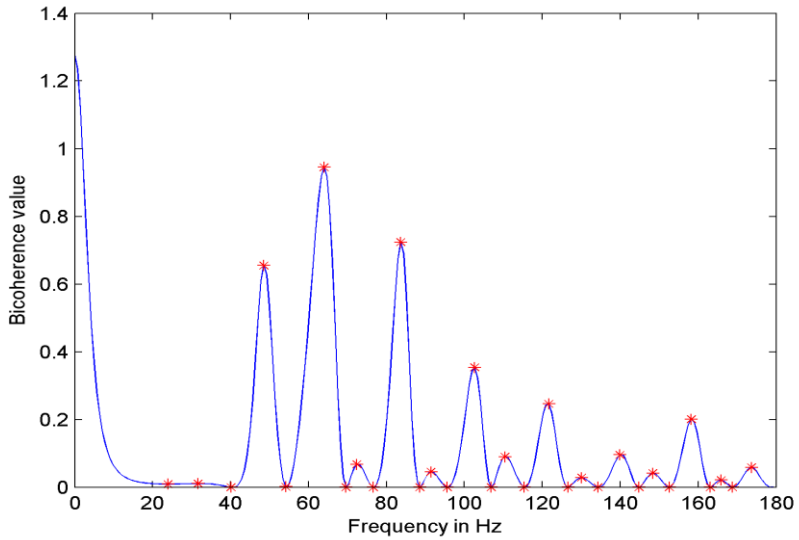

(c)

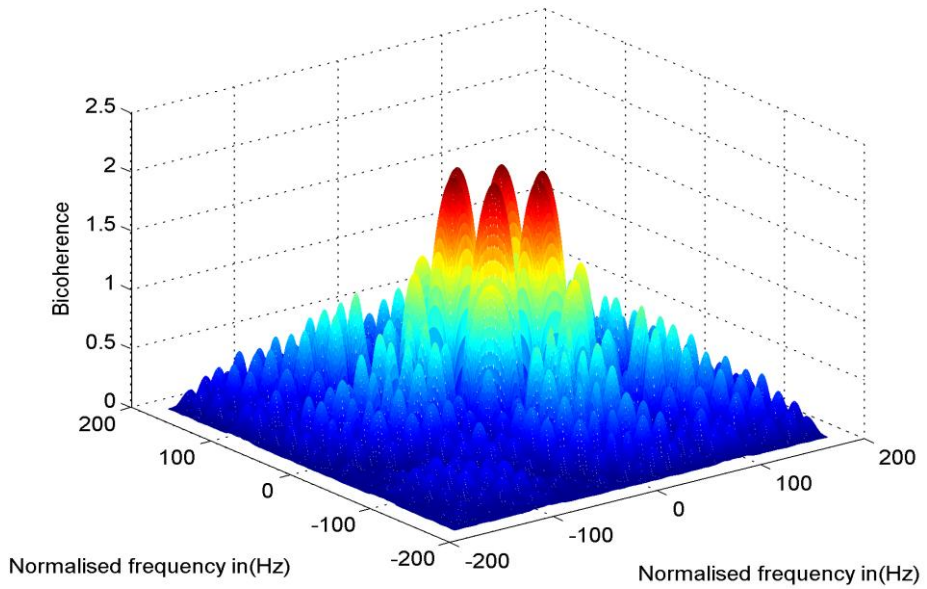

(d)

Figure 5.5 a. Bispectrum, b. Bicoherence c. Bicoherence selected peaks and d.3-D bicoherence plot for Apb beat

For the atrial premature beat, since the beats are premature and is very close to the normal it exhibit peaks at lower frequencies in the bispectrum. In the bicoherence most of the values are scattered also as in normal. Fig. 5.5 (c)

shows that the values are more concentrated at the center because of the atrial depolarisation, with the average bicoherence value at 2.1

From fig.5.1 through 5.5 we can see the difference between the normal and other arrythmias presented in the plots. The first 10 highest values of the bicoherence amplitude against their respective frequencies was used as another set of features, a 25x20 set of features was obtained and fed to neural network for training and 10x20 was use for testing the network and an average accuracy of 92% was obtained.

Table 5.2(a) Confusion matrix for the testing of features derived from the peaks of bicoherence

Signal	Normal	Rbbb	Paced	Lbbb	Apb
Normal	2	0	0	0	0
Rbbb	0	2	0	0	0
Paced	0	0	2	0	0
Lbbb	0	0	0	0	0
Apb	0	0	0	2	2

5.2(b) Table For the correctly and non correctly classified samples

Signal/parameter	TP	FP	TN	FN
Normal	2	0	8	0
Rbbb	2	0	8	0
Paced	2	0	8	0
Lbbb	0	2	8	0
Apb	2	0	6	2

Table 5.2c Performance matrix for the testing of features derived from the peaks of bicoherence and classified with ANN

Parameters	Normal	Rbbb	Paced	Lbbb	Apb	**%Ave.**
Sensitivity%	100	100	100	0	50	**70**
Specificity%	100	100	100	80	75	**91**
Positive pre.%	100	100	100	0	100	**80**
Accuracy%	100	100	100	80	80	**92**

5.3 Result with K-Nearest Neighborhood Search

In applying the knn search to our peaks set of features, we find out that we need more set of features in order to used this algorithm. Hence we developed a new set of samples from different signals and made our features for both training and testing to be a 50x20 matrix. After applying the principal component analysis we reduced the features to 11 from 20 and used 70% of the data for training which is 35x11while 30% was used for testing with 15x11 features. The figure below shows how the knn-neighborhood of the five classes which shows that the classes are not discriminated.

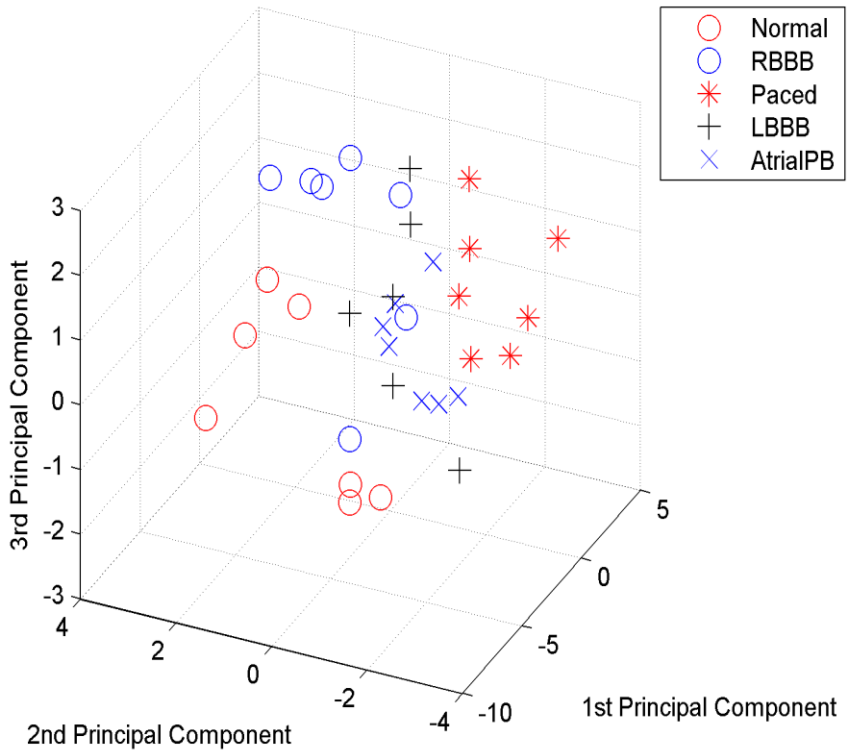

Figure 5.6 3-D plot for the principal component analysis showing the k-neighbors

The following performance measures were calculated.

Table 5.3a Confusion matrix for the testing of features derived from the peaks of bicoherence using knn-search

Signal	Normal	Rbbb	Paced	Lbbb	Apb
Normal	3	0	0	0	0
Rbbb	0	2	0	0	0
Paced	0	1	3	0	0
Lbbb	0	0	0	3	0
Apb	0	0	0	0	3

Table 5.3(b) Table For the correctly and non correctly classified samples

Signal/parameter	TP	FP	TN	FN
Normal	3	0	12	0
Rbbb	2	1	12	0
Paced	3	0	11	1
Lbbb	3	0	12	0
Apb	3	0	12	0

Table. 5.3c Performance matrix for the testing of features derived from the peaks of bicoherence using knn-search

Parameters	Normal	Rbbb	Paced	Lbbb	Apb	**%Average**
Sensitivity%	100	100	75	100	100	**95**
Specificity%	100	93.3	100	100	100	**98.7**
Positive pre.%	100	66.7	100	100	100	**93.3**
Accuracy%	100	93.3	100	100	100	**98.7**

Fig. 5.3d Comparison of performance matrix parameters for the three methods presented.

Parameters	Statistical parameters	Peaks using ANN	Peaks using Knn-search
Sensitivity%	88.4	70	95
Specificity%	96.2	91	98.3
Positive pre.%	94.9	80	93.3
Accuracy%	94.9	92	98.3

From the three methods presented above in this research, we can observe that by using the knn-search methods we obtained a better result with an average accuracy of up to 98.3%, using the neural network also gives an appreciable result, though the samples are not enough for a general conclusion. Spectral analysis classification is very effective in classifying the heart rate signal especially the one we developed here using the peaks of the bicoherence.

5.4 Comparison with Other Nonlinear Methods

A lot of work has been done in trying to classify the heart rate signal with higher order spectra and, the summary of their results is given in table 5.4

Fig. 5.4 Comparison of between the proposed method and other nonlinear approaches

Authors	Method	No of classes	Accuracy%
Acharya et. Al 2003	Non-linear features-ANN-fuzzy	4	95
Acharya et. Al 2003a	Non-linear fuzzy	8	85.36
Kannathal et. Al	Anfis	10	94.09
Chua et al	SVM	5	85.79
Acharya et al	AR,MA and ARMA modelling	9	83.38
Our first method	Statistical parameters with ANN	5	94.9
Second method	Bicoherence peaks using ANN	5	92
Third method	Bicoherence peaks using Knn-search	5	98.3

Acharya et al; pioneered this work on HRV classification using non-linear parameters such as spectral entropy, Poincare plot geometry and larger Lyapunov exponent. In their initial attempt they were able to achieve an average accuracy of 95% for four classes (Acharya et al; 2004b). Kannathal et al; have improved this work using adaptive neuro-fuzzy interference (ANFIS)

classifier and they were able to achieve a better efficiency of 94.09% (Kannathel et al; 2006).

Acharya et al; again classified cardiac states using modelling technique such as Auto regression (AR), moving average(MA) and Auto regression moving average (ARMA) into 9 classes (Acharya et al 2008a). They have used the first three peaks amplitude and corresponding peak frequencies as the features into neural network classifier. They obtained around 83.38% accuracy on HRV classification of cardiac conditions. In our methods we used five classes to classify another five cardiac condition with features derived from the first ten significant peaks amplitude of the bicoherence with their corresponding frequencies with two different classifiers and obtained a better result with the Knn-search algorithm given the best result with average accuracy of 98.3%, sensitivity and specificity of 95% and 98.3% respectively as compared to other nonlinear methods.

CHAPTER 6

CONCLUSION AND FUTURE WORK

6.0 Conclusions

The most important steps in ECG diagnosis is to detect and measure different waves, which form the entire ECG cycle, to extract efficient features and find a suitable structure and algorithm for the best classifier in ECG classification.

Therefore, the process of diagnosis usually requires meticulous study of the signals over a long period of time. This can be reduced considerably if computer based algorithms are used to identify, detect, and project the abnormalities, in the form of discriminating visual displays. The work of this research deals with the analysis, identification and display of ECG for the purpose of diagnosing cardiac abnormalities.

ECG signals are highly variable even among normal healthy persons; but the symptoms of disease are clear in its nature of variation. HOS analysis provides a visual pattern on the computer screen, which can be of considerable help in diagnostics. In this work we have proposed unique bispectrum and bicoherence plots for normal and four other cardiac abnormalities and they all varied visually. These plots are in some ways easier to interpret than power spectra where peak and frequencies of interest must be identified. The medical practitioners, who are not familiar with signal processing techniques, can easily interpret these plots for diagnosis. HOS plots are also better than time domain plots, because they can easily be compared on the screen with a reference and lend them better to the use of pseudo-colorings. In our work we have shown that HOS can serve to provide some indication that classifiers can be trained with their based features to perform automated classification.

Artificial intelligent tools, such as artificial neural network and knn-neighborhood search were used to identify the diseases given some certain parameters of the input signal. Though, helpful in diagnostics of cardiac

abnormalities, the reliability of these classifiers cannot be taken to be 100%, their accuracy depend upon on how best the network was trained.

In this work, an average accuracy of 94.9% have been achieved using the statistical features with artificial neural network as classifier and 98.3% using the significant peaks amplitude of the bicoherence with their corresponding frequencies.

6.1 Summary

Many aspects of healthcare require the processing and analysis of physiological signals such as electrocardiogram (ECG), electroencephalogram (EEG), electromayogram (EMG), heart rate variability (HRV) and medical images. This may require tasks such as noise reduction, feature extraction/detection, pattern analysis/classification, visualization and modeling. Some of the inherent characteristics of biomedical signals are non-linearity, non-stationarity, non-Gaussianity, uncertainty and imprecision.

Bio-signals are essential non-stationary signals. They often, display a fractal like self-similarity. They may contain indicators of current disease, or even warnings about impending diseases. The indicators may be present at all times or may occur at random-in the scale. However, to (study) and pinpoint anomalies in voluminous data collected over several hours is strenuous and time consuming.

Therefore, a robust analytical tool for in depth study and classification of data collected over long intervals can be very useful in diagnostics. These HOS based nonlinear dynamical techniques are based on chaos theory and have been applied to many areas which include the areas of medicine and biology.

In this study HOS have been used to classify normal heart rate with four other diseases using both statistical and peak features of the higher order spectra.

Although, the data set used for HOSA features is a small set, the higher order spectral features, is a promising method for classification of ECG arrhythmias.

6.2 Advantages and Disadvantages of the Proposed Method

Some of the advantages of this method are:

- ECG signal are nonlinear, non-Gaussian and non-stationary, hence HOS method gives the phase information about the signal.
- HOS method gives us visual aid in interpreting the arrhythmias.
- HOS methods used in this work achieved a very high accuracy of 98.3% compared to other nonlinear algorithm.

The disadvantage of this method may be an accurate feature extraction for HOSA, bicoherence should be at least 1min of the signal sample.

6.3 Future Directions

The future direction of higher order spectra research can be in the following:

- Exploring more channels of the signal, since we only use one signal in this work, extending the work to cross-bispectral and cross-bicoherence for ECG at different channels
- Is possible to try and detect the QRS with HOS technique
- Further investigation of features from HOS is possible

BIBLIOGRAPHY

Abeyratne U. R., Petropulu A. P. and Raid J. M., 1995, Higher Order Spectra Based Deconvolution Of Ultrasound Images. IEEE Transactions on ultrasonic, Ferroelectronics and Frequency Control. Vol. 42(6), pp. 1064-1075.

Acharya U. R., Bhat P.S, Iyengar S. S.,Rao A. and Dua S., 2003, Classification of heart rate data using Artificial neural networks and fuzzy equivalence relations. J. Pattern Recognition, Vol. 36(1), pp. 61-68.

Acharya U. R., Kannathal N. and Krishan S. M. 2004(a), Comprehensive analysis of Cardiac Health using heart rate signal. Phisiological Measurement, UK, Vol. 25, pp.1130-1151.

Acharya U. R., Kumar Ashwin, Bhat Subbanna P., Iy1engar S. S. Kannathal N. and Krishan, 2004(b), Classification of Cardiac Abnormalities using heart rate signal. IFMBE Journal of Medical & Biological Engineering and Computing, Vol. 42(3), pp. 288-293.

Acharya U. R., Meena S. Nayak J., Xiang C. and Tamura T., 2008(a), Automatic Identification of Cardiac Health using Modeling Techniques: A Comparative Study. Infor. Sceinces, Vol. 178(33), pp. 4571-4582.

Berne, R. and Levy M., 1997, Cardiovascular Phisiology, 7th Edition.

Brillinger, D. R and Rosenblatt. M., 1967, Computation and Interpretation of k-th Order Spectra,In Harris B, Editor. Spectral Analysis of Time-Series. New York: Wiley, pp.189- 232.

Broomhead D. S. and King G. P., 1987, Extracting Qualitative Dynamics From Experimental Data. Phisica D. Vol. 20, pp. 217.

Chandran V., Elgar S. and Pezeshki C., 1993(b), Bispectral and Trispectral Characterization of Transient to Chaos in the Duffing Oscillator. Intl. Journal of Bifurcation and Chaos, Vol. 3(3), pp. 551-557.

Chandran V., Elgar S. and Vanhoff B., 1994, Statistics of Tricoherence. IEEE Trans. On sp, Vol. 42(12), pp. 3430-3440.

Chandran V., Elgar S. and Nguyen A., 2002, Detection of Mine in Acoustic Images Using Higher Order Spectral Features, IEEE. Journal ocean Eng. Vol. 27(3), pp. 610-618.

Chandran V., Sridharan S., 2004, Recognition using Higher Order Spectral Phase Features and Their Effectiveness vis-à-vis Mel Cepstral Features, Lecture notes in Computer Science (3072), pp. 614-622.

Chua K. C., Chandran V., Acharya U. R., Ng E. Y. K., Chee C., Gupta M., Lim C. M., Mellisa T. Y. J., Gracielynne F. and Surij. S., 2007, Computer based detection of Diabetes Micalopathy Stage using Higher Order Spectra, Image Modeling of Human Eye eds Acharya et al, Artech House.

Chua K. C., 2010, Analysis of Cardiac and Epileptic Signals using Higher Order Spectra, A Phd Thesis Submitted to Queensland University of Technology.

Cooper P J., Lei M., Cheng L. X. and Kohl P., 2000, Selected Contribution: Axial Stretch Increases Spontaneous Pacemaker Activity in Rabbit Isolated Sino atrial cells, Journal Applied Phisiology, Vol. 89(5).

Danker M. and Keller G., 1986, Rigorously Statistical Procedures for Data from Dynamical Systems, Stat. Phys. Vol.44, pp. 67.

De La Rosa J., Moreno A., Puntonet c. G. and Gorriz J. M., 2007, Higher Order Spectral Characterization of Termite Emission using Acoustic Emission Probes, IEEE Sensors Applications Symposium SAS 107, pp. 1-6.

Elgar S. and Guza R. T., 1995, Statistics of Bicoherence, IEEE Trans. On Assp, Vol. 36(10), pp. 1667-1668.

El-Jaroudi A., Akgul T. and Siman M., 1994, Application of Higher Order Spectra to Multi-scale Deconvolution of Sensor Arrays Signal, Proceedings of IEEE International Conference on Acoustics, Speech and Signal Processing, pp. 413-416.

El-Khamy S. E., Ali A. F. and El-Ragal H. M., 1995, Fast Blind Equalization using Higher Order Spectra Channel Estimation in The Presence of Severe ISI, Proceedings, IEEE Symposium in Computers and Communications, pp. 248-254.

Fackrell J. W. A., P. R. White., J. K. Hammond., R. J. Pinnington and A. T. Parsons., 1995, The Interpretation of the Biapectra of Vibration Signals-1.theory. Mechanical System and Signal Processing 9, pp. 257-266.

Friensen G. M., Thomas C. J., Jadallah M. A., Yates S. L., Quint S. R. and Nagle H. T., 1990, A Comparison of Noise Sensitivity of a QRS Detection Algorithms, IEEE Trans. Bimed. Eng. Vol. 37(1), pp. 85-98.

Garret D., Peterson D. A., Anderson C. W. and Thaut M. H., 2003, Comparison of Linear and Nonlinear Methods for EEG Signal Classification, IEEE Transactions on Neural Systems and Reliabilitative Engineering, Vol. 11(2), pp. 141-144.

Guckenheimer J. and Holmes P., 1983, Nonlinear Oscillations, Dynamical System and Bifurications of Vectors Fields, Springer- Verlag:Berlin.

Hasselman K., Munk W., and Macdonald G., 1963, Bispectra of Ocean Waves, Tme-Series analysis, Rosenblatt M. Ed. New York: Wiley, pp. 125-139.

Hinich M. J., 1982, Testing of Gaussianity and Linearity of a Stationary Time-Series, Time-Series Analysis, pp. 169-176.

Husar P. and Henning G., 1997, Bispectrum Analysis of Visually Evoked Potentials, IEEE Engineering in Medicine and Biology, pp. 57-63.

Holter N. J., 1961, New Methods for Heart Studies: Continuous Electrocardiography of Active Subjects, Science, Vol. 134, pp, 1214-1220.

J. Malmivuo and R. Plunsey., 1995, Bioelectromagnetism: Principles and Applications of Bioelectric and Biomagnetic Fields, Oxford University Press, 1st Edition.

Kannathal N., Acharya U. R., Fadilah A., Thalma T. and Sidasivan P. K., 2004, Nonlinear Analysis of EEG Signals At Different Mental States, Biomedical Online Journal.

Kaplan A. Y., 1999, Segmental Structure of EEG More Likely Reveals the Dynamic Multi-stability of the Brain Tissue than the Continual Plasticity one, Proceedings of KONIP, Perth, Australia, pp. 633-638.

Khadra L.,Al-Fahoum A. S. and Binajjaj S., 2005, A Qualitative Analysis and Approach for Cardiac Arrhythmia Classification using Higher Order Spectral Techniques, IEEE Trans. Biomedical Engineering, Vol. 52(11), pp. 1840-1845.

Laurent H., and Doncali C., 2000, Stationary Index for Abrupt Changes Detection in the Time Frequency Plane, IEEE Signal Processing Letters, Vol. 5(2), pp. 43-45.

MIT Arrhythmia Database Available From: http://www.phisionet.org/phisiobank/database/mitdb

Nikias C. L. and Rughuveer M. R., 1987, Bispectrum Estimation: A Digital Signal Processing Framework, Proce. IEEE, Vol. 75, pp. 869-890.

Nikias C. L. and Petropulu A. P., 1993(b), Higher Order Spectral Analysis: A Nonlinear Signal Processing Framework, Englewood Cliff, HJ, PTR Prentice Hall.

Ning T. and Bronzino J. D., 1990, Autoregressive and Bispectral Analysis Techniques: EEG Applications, IEEE Engineering in Medicine and Biology Magazine, Vol. 9(1), pp. 47-50.

Ning T., 1993, Nonlinear Analysis of the Hippocanpal Subfields of CAI and the Dentate Gyrus, IEEE Transactions on Biomedical Engineering, Vol. 40(9), pp. 870-876.

Ong H. and Chandran V., 2005, Identification of Gastroenteric Viruses by Electron Microscopy using Higher Order Special Features, Journal of Clinical Virology, No.3, pp. 195-206.

Ozbey, Y., Karlik, B., 1996 A New Approach for Arrhythmias Classification, Proc. of Annual International Conference of IEEE of Medicine and Biology Society.

Pan J. and Thompkins W. J., 1985, A Real-Time QRS Detection Algorithm, IEEE Trans. Biomed. Eng. Vol. 32, pp. 230-236.

Valupadasu R., B. Ramarao C. and Venkanna C., 2012, Identification of Cardiac Ischemia Using Bispectral Analysis of ECG, IEEE EMBS, International Conference on Biomedical Engineering and Sciences, Langkawi.

Roberto D., 1995, Segmentation of Brain Electrical Activity into Micro states: A Model Estimation and Validations, IEEE Transactions on Biomedical Engineering, Vol. 42(7), pp. 658-638.

Shen M., F. H. Y., Sun L. and B. J., 2000, Parametric Bispectral Estimation of EEG Signals in Different Functional States of the Brain, IEEE Proc. In Science Measurement and Technology, Vol. 147(6), pp. 374-377.

Simm C. W., Sawley M. L., Skiff F. and Pochelon A., 1987, On the Analysis for Experimental Signals for Evidence of Deterministic Chaos, Helv. Phys. Acta, Vol. 60, pp. 510.

Schetza M., 1980, The Volterra and Wiener Theories of Nonlinear Systems, New York, NY: Wiley.

Swami A., mandel C. M and Nilias C. L., 2000, Higher Order Spectral Analysis (HOSA) Toolbox, Version 2.0.3.

Webster J. G., 1993, Design of Cardiac Pacemakers, Tab-IEEE Press.

Webster J. G., 1998 Medical Instrumentation, Application and Design, Houghton, Miffin Company, 3rd Edition.

Yanowitz F. G., 2006, ECG Learning center in Cyberspace, Available on the Web at http://library.med.uteh.edu/kw/eeg/index.html.

Yuru Z., Wang H., Ju K. M. and Chu K. H., 2004, Nonlinear Analysis of Separate Contributions of Autonomic Nervous Systems to Heart Rate Variability using Principal Dynamic Modes, IEEE Transactions on Bio. Eng. Vol. 5(2), pp. 255-260.

APPENDICES

APPENDIX A: Matlab codes

The comprehensive Matlab code used in this thesis is in the attached DVD for further reference.